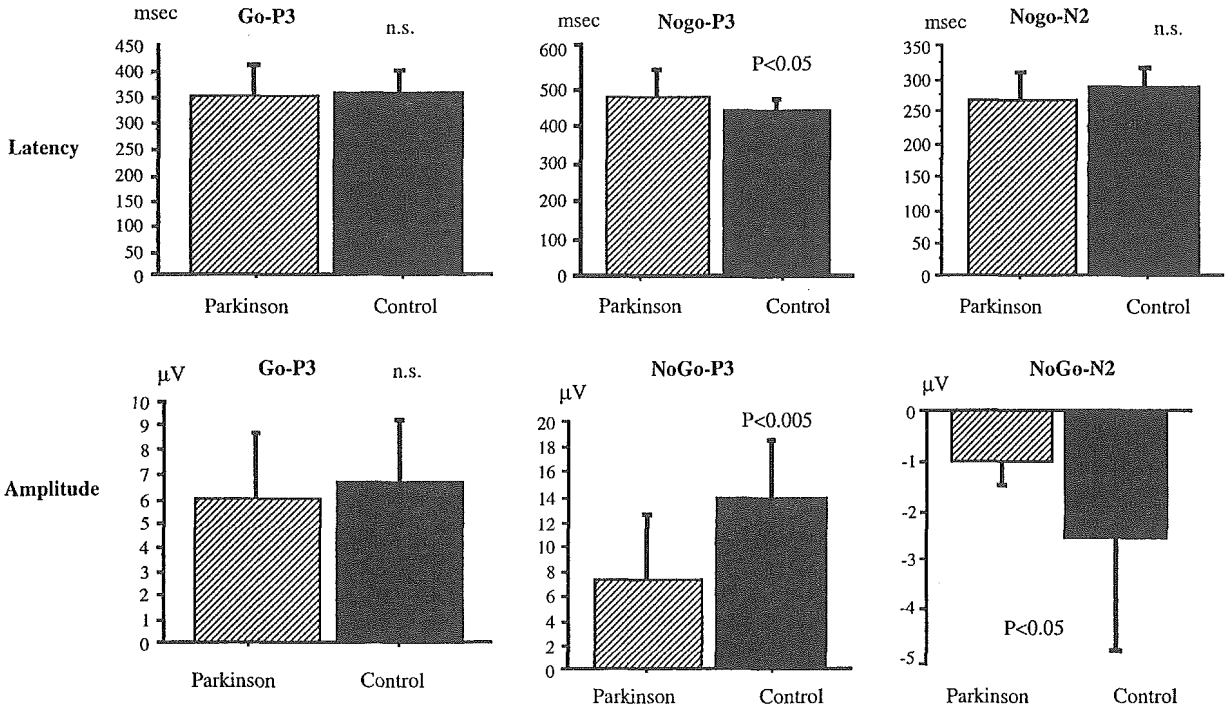

Fig. 2. Latencies and amplitudes for the Go-P3, NoGo-P3, and NoGo-N2 in the PD and control groups. Values are the mean ± S.D.

ment (r) or Spearman's rank order correlation coefficients (R). A level of $p<0.05$ was accepted as statistically significant, and the significance level was adjusted using the Greenhouse–Geisser correction when appropriate. The original degree of freedom and its epsilon value were reported.

3. Results

3.1. Performance

The average error rate in the PD group was 12.2 ± 8.2% (mean ± S.D.) for omission errors (misses) and 11.5 ± 8.2% for commission errors (false alarms). The control group values were 3.5 ± 2.9 and 1.5 ± 1.5%, respectively. The PD group had higher error rates than did the control group (omission error: $F_{(1,25)}=10.6$, $p<0.005$; commission error: $F_{(1,25)}=11.1$, $p<0.005$). However, the reaction times for correct responses did not differ between the two groups; they were 449.0 ± 85.6 ms for the PD group and 438.5 ± 74.5 ms for the control group.

3.2. ERP components

Fig. 1 shows the electrode locations and actual ERP waveforms at the electrode sites where the maximum amplitude was obtained for each component (Ch 80 for Go-P3, Ch 13 for NoGo-P3, and Ch 4 for NoGo-N2), and Fig. 2 shows the latencies and amplitudes for the Go- and NoGo-P3 and NoGo-N2 in the PD and control groups. There were no differences in the Go-P3 latency and amplitude between the two groups. By contrast, the latency of NoGo-P3 for the PD group was longer than that for the control group (478.8 ± 66.4 versus 431.7 ± 36.8 ms, $F_{(1,25)}=5.13$, $p<0.05$). The amplitudes of NoGo-P3 and NoGo-N2 were also smaller for the PD group than for the control group (7.3 ± 5.2 μV versus 13.8 ± 4.7 μV, $F_{(1,25)}=10.2$, $p<0.005$ for NoGo-P3, −1.0 ± 0.5 μV versus −2.6 ± 2.3 μV, $F_{(1,25)}=5.37$, $p<0.05$ for NoGo-N2).

3.3. Scalp topography

Fig. 3 shows the interpolated voltage maps for the Go-P3, NoGo-P3, and NoGo-N2 over the scalp surface. With regard to the Go-P3 component, the maximum amplitude was found over the centroparietal area in both the PD and control groups (main anterior–posterior effect, $F_{(3,75)}=15.2$, $\varepsilon=0.49$, $p<0.0001$; interaction of anterior–posterior × group, $F_{(3,75)}=2.0$, $\varepsilon=0.46$, $p=0.12$). Conversely, the NoGo-P3 peaked in the frontocentral area. The anterior shift of the NoGo-P3 peak was highly significant compared with the Go-P3 topography (interaction of task condition × anterior–posterior, $F_{(3,75)}=45.0$, $\varepsilon=0.56$, $p<0.0001$), and this anterior distribution of NoGo-P3 was comparable in the PD and control groups (interaction of anterior–posterior × group, $F_{(3,75)}=1.15$, $\varepsilon=0.53$, $p=0.32$). There were no topographic differences between the PD and control groups for either the Go- or NoGo-P3 topographies (interaction of group × hemisphere × latitude × anterior–posterior,

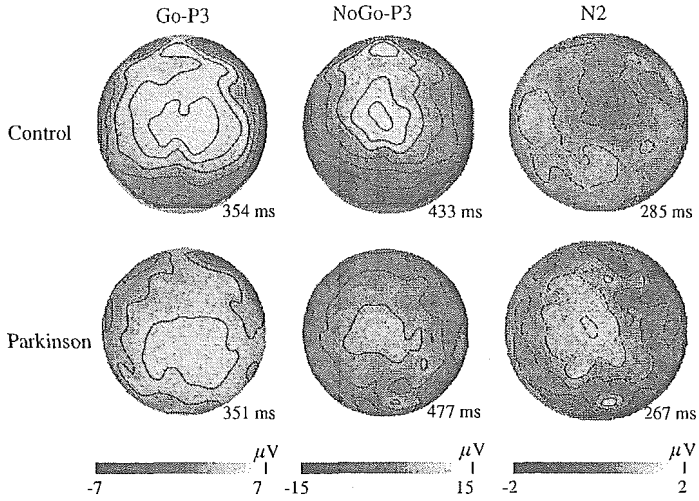

Fig. 3. The interpolated voltage maps of the Go-P3, NoGo-P3, and NoGo-N2 over the scalp surface in the PD and control groups. The map is presented at the peak latency for each component.

$F_{(3,75)} = 0.69$, $\varepsilon = 0.68$, $p = 0.51$ for Go-P3; $F_{(3,75)} = 0.93$, $\varepsilon = 0.79$, $p = 0.41$ for NoGo-P3). The maximum amplitude of NoGo-N2 was over the frontal area (main anterior–posterior effect, $F_{(3,75)} = 5.39$, $\varepsilon = 0.47$, $p < 0.05$). This scalp distribution was the same in the PD and control groups (interaction of anterior–posterior × group, $F_{(3,75)} = 2.02$, $\varepsilon = 0.47$, $p = 0.16$).

3.4. Cognitive functions

There were no significant differences in the HDS-R scores for the PD and control groups (PD group: 26.1 ± 2.6, control group: 27.8 ± 2.8). By contrast, the WCST was impaired in the PD group compared with the controls (PD group: 2.1 ± 2.4, control group: 4.9 ± 1.4, $Z = 2.56$, $p < 0.005$). The Verbal Fluency Test and Kana Pick-out Test were also impaired in the PD group (PD group: 3.8 ± 2.5, control group: 7.1 ± 3.2, $F_{(1,25)} = 5.31$, $p < 0.05$ for the Verbal Fluency Test; PD group: 13.6 ± 11.7, control group: 30.7 ± 12.3, $F_{(1,25)} = 5.18$, $p < 0.05$ for the Kana Pick-out Test).

3.5. Correlation between ERP components and cognitive functions

Table 2 shows the correlations between the ERP measures and the scores of the various tests of cognitive function for all subjects. The NoGo-P3 latency was correlated with the Kana Pick-out Test ($r = -0.49$, $p < 0.05$) and Verbal Fluency Test ($r = -0.55$, $p < 0.02$), while the NoGo-P3 amplitude was correlated with the Verbal Fluency Test ($r = 0.54$, $p < 0.01$) and WCST ($R = 0.70$, $p < 0.005$). We also conducted the correlation analysis within the PD group. There were still some correlations between NoGo-P3 and test scores; the NoGo-P3 latency was correlated with the Verbal Fluency Test ($r = -0.69$, $p < 0.05$), and the amplitude was correlated with WCST ($R = 0.73$, $p < 0.01$). Conversely, neither the latency nor the amplitude of the Go-P3 was correlated with any cognitive function tests. Similarly, neither the latency nor the amplitude of the NoGo-N2 was correlated with any cognitive functions.

We also performed correlation analyses between commission errors and ERP measures. The number of commission errors was significantly correlated with the NoGo-P3 latency ($r = 0.49$, $p < 0.01$) and NoGo-P3 amplitude ($r = -0.59$, $p < 0.01$) for all subjects. When the correlation analysis was performed only in the PD group, the number of commission errors was still correlated with the NoGo-P3 amplitude ($r = -0.55$, $p < 0.05$) and NoGo-N2 amplitude ($r = 0.58$, $p < 0.05$; note that the N2 amplitude is a negative value). The Go-P3 measures did not show any correlations with commission errors. Furthermore, the number of commission errors

Table 2
Correlations between ERP measures and cognitive functions

	Hasegawa test (r)	Kana pick-out test (r)	Verbal fluency test (r)	WCST (R)
Go-P3 latency	−0.21	−0.23	−0.11	−0.03
Go-P3 amplitude	0.11	0.12	0.41	−0.21
NoGo-P3 latency	−0.37	−0.49*	−0.55*	−0.32
NoGo-P3 amplitude	0.55*	0.25	0.54*	0.70**
NoGo-N2 latency	0.26	0.12	−0.18	0.27
NoGo-N2 amplitude	−0.25	−0.29	−0.15	−0.25

WCST: Wisconsin Card Sorting Test, r: Pearson's product-moment correlation coefficient, R: Spearman's rank order correlation coefficient.
* $p < 0.05$.
** $p < 0.01$.

was correlated with frontal function test scores across both groups ($R = -0.69, p < 0.001$ for WCST; $R = -0.63, p < 0.005$ for the Kana Pick-out Test; $r = -0.56, p < 0.01$ for the Verbal Fluency Test) and with some test scores for the PD group ($R = -0.68, p < 0.01$ for the WCST; $R = -0.85, p < 0.001$ for the Kana Pick-out Test).

4. Discussion

The PD group had significantly greater error rates than did the control group, but there was no significant group difference in reaction times. Most previous studies of simple or choice reaction tasks have reported general impairments in patients with PD. Tachibana, Aragane, Miyata, and Sugita (1997) reported that PD patients performed a simple reaction task normally, but the reaction time was significantly slower for a Go/NoGo discrimination task. We found no delay in the reaction time for the Go/NoGo task in the PD group, but the error rate was higher in the PD group than in the control group. Specifically, the higher rate of false alarms may account for the absence of a prolonged reaction time in the PD group because of a trade-off between reaction time and commission error.

The latency and amplitude of Go-P3 did not differ significantly between the two groups. It has been suggested that PD patients can perform a simple reaction task without difficulty. Furthermore, we demonstrated that neither the latency nor the amplitude of Go-P3 was correlated with any measures of the cognitive function tests. Several authors have reported that medicated patients with PD have a prolonged P3 latency (Hansch et al., 1982; Prasher & Findley, 1991; Rumbach, Tranchant, Viel, & Warter, 1993), while others have demonstrated normal P3 latency (Ebmeier et al., 1992; Karayanidis, Andrews, Ward, & Michie, 1995; Stanzione et al., 1991; Tachibana et al., 1992; Toda, Tachibana, Sugita, & Konishi, 1993). This discrepancy might result from differences in the task or the degree of cognitive impairment in the patients.

All of our patients were being treated with L-dopa and other anti-Parkinson drugs, which might have affected their cognitive functions. Delayed N2 and P3 latencies have been reported in untreated PD patients (Prasher & Findley, 1991; Sohn, Kim, Huh, & Kim, 1998). While anticholinergic drugs are thought to impair the immediate recognition of information, the effect of L-dopa on cognitive functions in PD is relatively small (Pillon et al., 1989). Stern, Mayeux, and Cote (1984) reported that attentional deficits in PD patients were correlated with an impaired subcortical frontal noradrenergic system. More detailed data are necessary to accurately assess the effects of drugs on cognitive functions in PD patients.

The most significant finding of this study is that PD patients had prolonged latency and lower amplitude of the NoGo-P3 and lower amplitude of the NoGo-N2 accompanied with normal Go-P3 measures. Whether NoGo-P3 and NoGo-N2 actually reflect the inhibitory mechanism must be addressed. One concern with this study is that the probability of NoGo trials was 30% in our paradigm. It is known that the probability of events influences the ERP amplitude, i.e., events with a lower probability generate a larger P3 component. The NoGo ERP measures might have been affected by the probability effect as well as the inhibition effect. Therefore, it is possible that the changes in the NoGo ERPs resulted from a reduced probability effect in PD patients. However, the finding that NoGo ERP measures were correlated with the number of commission errors and frontal function test scores suggests a significant influence of inhibitory processes on NoGo ERPs. Another concern is that our paradigm requires working memory for correct performance because the subjects had to keep the digit "3" in mind while considering the following two digits. Therefore, it is possible that working memory deficits in PD impaired performance in the NoGo trials. This possibility is also unlikely because only NoGo ERPs were affected in PD patients, although the working memory load was comparable in the Go and NoGo trials.

The WCST requires a set-shifting process, which is functionally linked to inhibitory function and anatomically related to the dorsolateral prefrontal cortex in humans (Milner, 1963). The Kana Pick-Out Test requires working memory and an executive process, which excludes distracter characters from the stimulus array, so this test is also thought to be a test of frontal lobe function (Inoue et al., 2003). We found significant correlations between NoGo-P3 measures and these frontal lobe function tests. Moreover, the correlation between commission errors and NoGo-P3 measures was also demonstrated in PD patients, as well as in all subjects. These findings support the notion that the NoGo-P3 is a valuable electrophysiological index for investigating inhibitory function related to the frontal lobe. Additional direct evidence for Nogo-P3 involvement in response inhibition was provided by a recent ERP study (Bruin, Wijers, & van Staveren, 2001); they reported that response priming in NoGo trials affected the P3 amplitude exclusively. Several reports support the hypothesis that the visual NoGo-N2 reflects a frontal inhibition mechanism (Falkenstein et al., 1999; Jodo & Kayama, 1992; Kok, 1986; Kopp et al., 1996; Ritter, Simson, Vaughan, & Macht, 1982). Kaiser et al. (2003) reported that depressed patients had reduced early frontotemporal positivity in the N2 time window, with a normal P3 in the NoGo task. In addition, the same group reported that schizophrenic patients had normal neural activity in the N2 time window, but lacked P3 lateralization in the NoGo task (Weisbrod, Kiefer, Marzinzik, & Spitzer, 2000). Our study demonstrated that the test scores for frontal cognitive functions were selectively correlated with the NoGo-P3 component. Although the two components of the NoGo-N2 and NoGo-P3 might reflect different stages of inhibitory information processing, the NoGo-P3 would be a more useful measure for studying inhibitory function in PD patients.

Weisbrod et al. (2000) reported that the NoGo-P3 component was generated from the left frontal lobe. We previously demonstrated that the main NoGo-P3 source was located in

the left orbitofrontal cortex in normal young adults, and the NoGo-N2 source was located in a right frontocentral site (Bokura et al., 2001), suggesting that there are different neuronal subsystems in the inhibitory mechanism. A recent fMRI study revealed that NoGo trials activated the orbitofrontal cortex and that the activity was correlated with behavioral performance (Casey et al., 1997). Non-human primate studies have also provided evidence for inhibitory control function in the orbitofrontal cortex (Fuster, 2000). Neurobehavioral studies in patients with orbitofrontal cortex damage owing to a closed head injury or cerebrovascular accident frequently show abnormal social behavior, such as disinhibited or socially inappropriate behavior (Starkstein & Robinson, 1997). These results suggest that the frontal lobe, including the orbitofrontal cortex, is involved in the NoGo-P3 response. Our study supports the hypothesis that PD patients have selective impairments of the inhibitory mechanism involved in frontal lobe function. The latency and amplitude of the NoGo-P3 appear to be valuable parameters for studying inhibitory deficits in PD patients.

Acknowledgments

This work was supported by a grant from the Japanese Ministry of Education, Culture, Sports, Science, and Technology (11670626) and by Medical Research Grants from the Shimane Institute of Health Science.

References

Aotsuka, A., Weate, S. J., Drake, M. E. J., & Paulson, G. W. (1996). Event-related potentials in Parkinson's disease. *Electromyography and Clinical Neurophysiology, 36*, 215–220.

Bench, C. J., Frith, C. D., Grasby, P. M., Friston, K. J., Paulesu, E., Frackowiak, R. S., et al. (1993). Investigations of the functional anatomy of attention using the Stroop test. *Neuropsychologia, 31*, 907–922.

Benton, A. L., Hamsher, K., Verney, N. R., & Spreen, D. (1983). *Contributions to Neuropsychological Assessment*. New York: Oxford University Press.

Bokura, H., Yamaguchi, S., & Kobayashi, S. (2001). Electrophysiological correlates for response inhibition in a Go/NoGo task. *Clinical Neurophysiology, 112*, 2224–2232.

Brown, R. G., & Marsden, C. D. (1990). Cognitive function in Parkinson's disease: From description to theory. *Trends in Neuroscience, 13*, 21–29.

Bruin, K. J., Wijers, A. A., & van Staveren, A. S. J. (2001). Response priming in a go/nogo task: Do we have to explain the go/nogo N2 effect in terms of response activation instead of inhibition? *Clinical Neurophysiology, 112*, 1660–1671.

Buchsbaum, M. S., Nuechterlein, K. H., Haier, R. J., Wu, J., Sicotte, N., Hazlett, E., et al. (1990). Glucose metabolic rate in normals and schizophrenics during the Continuous Performance Test assessed by positron emission tomography. *British Journal of Psychiatry, 156*, 216–227.

Cabeza, R., & Nyberg, L. (2000). Imaging cognition II: An empirical review of 275 PET and fMRI studies. *Journal of Cognitive Neuroscience, 12*, 1–47.

Carter, C. S., Mintun, M., Nichols, T., & Cohen, J. D. (1997). Anterior cingulate gyrus dysfunction and selective attention deficits in schizophrenia: $[^{15}O]H_2O$ PET study during single-trial Stroop task performance. *American Journal of Psychiatry, 154*, 1670–1675.

Casey, B. J., Trainor, R. J., Orendi, J. L., Schubert, A. B., Nystrom, L. E., Giedd, J. N., et al. (1997). A developmental functional MRI study of prefrontal activation during performance of a go–no go task. *Journal of Cognitive Neuroscience, 9*, 835–847.

Charbonneau, D., Riopelle, R. J., & Beninger, R. J. (1996). Impaired incentive learning in treated Parkinson's disease. *The Canadian Journal of Neurological Sciences, 23*, 271–278.

Dias, R., Robbins, T. W., & Roberts, A. C. (1997). Dissociable forms of inhibitory control within prefrontal cortex with an analog of the Wisconsin Card Sort Test: Restriction to novel situations and independence from "on-line" processing. *Journal of Neuroscience, 17*, 9285–9297.

Ebmeier, K. P., Potter, D. D., Cochrane, R. H., Crawford, J. R., Stewart, L., Calder, S. A., et al. (1992). Event related potentials, reaction time, and cognitive performance in idiopathic Parkinson's disease. *Biological Psychology, 33*, 73–89.

Eimer, M. (1993). Effects of attention and stimulus probability on ERPs in a Go/Nogo task. *Biological Psychology, 35*, 123–138.

Falkenstein, M., Hoormann, J., & Hohnsbein, J. (1999). ERP components in Go/Nogo tasks and their relation to inhibition. *Acta Psychologica, 101*, 267–291.

Fallgatter, A. J., Mueller, T. J., & Strik, W. K. (1999). Age-related changes in the brain electrical correlates of response control. *Clinical Neurophysiology, 110*, 833–838.

Fallgatter, A. J., & Strik, W. K. (1997). Right frontal activation during the continuous performance test assessed with near-infrared spectroscopy in healthy subjects. *Neuroscience Letters, 223*, 89–92.

Fallgatter, A. J., & Strik, W. K. (1999). The NoGo-anteriorization as a neurophysiological standard-index for cognitive response control. *International Journal of Psychophysiology, 32*, 233–238.

Ferree, T. C., Luu, P., Russell, G. S., & Tucker, D. M. (2001). Scalp electrode impedance, infection risk, and EEG data quality. *Clinical Neurophysiology, 112*, 536–544.

Franz, E. A., & Miller, J. (2002). Effects of response readiness on reaction time and force output in people with Parkinson's disease. *Brain, 125*, 1733–1750.

Fuster, J. M. (2000). Executive frontal functions. *Experimental Brain Research, 133*, 66–70.

Garavan, H., Ross, T. J., & Stein, E. A. (1999). Right hemispheric dominance of inhibitory control: An event-related functional MRI study. *Proceedings of the National Academy of Sciences of the United States of America, 96*, 8301–8306.

Gauggel, S., Rieger, M., & Feghoff, T. A. (2004). Inhibition of ongoing responses in patients with Parkinson's disease. *Journal of Neurology, Neurosurgery, and Psychiatry, 75*, 539–544.

Geczy, I., Czigler, I., & Balazs, L. (1999). Effects of cue information on response production and inhibition measured by event-related potentials. *Acta Physiologica Hungarica, 86*, 37–44.

Gotham, A. M., Brown, R. G., & Marsden, C. D. (1988). 'Frontal' cognitive function in patients with Parkinson's disease 'on' and 'off' levodopa. *Brain, 111*, 299–321.

Hansch, E. C., Syndulko, K., Cohen, S. N., Goldberg, Z. I., Potvin, A. R., & Tourtellotte, W. W. (1982). Cognitionin Parkinson disease: An event-related potential perspective. *Annals of Neurology, 11*, 599–607.

Hoehn, M. M., & Yahr, M. D. (1967). Parkinsonism: Onset, progression and mortality. *Neurology, 17*, 427–442.

Iijima, M., Osawa, M., Ushijima, R., & Iwata, M. (1999). Nogo event-related potentials in Parkinson's disease. *Electroencephalography and Clinical Neurophysiology, 49*(Suppl.), 199–203.

Inoue, M., Suyama, A., Kato, T., Urakami, K., Nakashima, K., & Meshitsuka, S. (2003). Development of computerized Kana Pick-out Test for the neuropsychological examination. *Computer Methods and Programs in Biomedicine, 70*, 271–276.

Jodo, E., & Kayama, Y. (1992). Relation of a negative ERP component to response inhibition in a Go/No-go task. *Electroencephalography and Clinical Neurophysiology, 82*, 477–482.

Kaiser, S., Unger, J., Kiefer, M., Markela, J., Mundt, C., & Weisbrod, M. (2003). Executive control deficit in depression: event-related potentials in a Go/Nogo task. *Psychiatry Research, 122*, 169–184.

Karayanidis, F., Andrews, S., Ward, P. B., & Michie, P. T. (1995). ERP indices of auditory selective attention in aging and Parkinson's disease. *Psychophysiology, 32*, 335–350.

Kok, A. (1986). Effects of degradation of visual stimulation on components of the event-related potential (ERP) in go/nogo reaction tasks. *Biological Psychology, 23*, 21–38.

Konishi, S., Nakajima, K., Uchida, I., Sekihara, K., & Miyashita, Y. (1998). No-go dominant brain activity in human inferior prefrontal cortex revealed by functional magnetic resonance imaging. *European Journal of Neurosciences, 10*, 1209–1213.

Kopp, B., Mattler, U., Goertz, R., & Rist, F. (1996). N2, P3 and the lateralized readiness potential in a nogo task involving selective response priming. *Electroencephalography and Clinical Neurophysiology, 99*, 19–27.

Labutta, R. J., Miles, R. B., Sanes, J. N., & Hallett, M. (1994). Motor program memory storage in Parkinson's disease patients tested with a delayed response task. *Movement Disorders, 9*, 218–222.

McCarthy, G., & Wood, C. C. (1985). Scalp distributions of event-related potentials: An ambiguity associated with analysis of variance models. *Electroencephalography and Clinical Neurophysiology, 62*, 203–208.

Milner, B. (1963). Effects of different brain lesions on card sorting. *Archives of Neurology, 9*, 90–100.

Pascual-Leone, A., & Hallett, M. (1994). Induction of errors in a delayed response task by repetitive transcranial magnetic stimulation of the dorsolateral prefrontal cortex. *Neuroreport, 5*, 2517–2520.

Perrin, F., Pernier, J., Bertrand, O., & Echallier, J. F. (1989). Spherical splines for scalp potential and current density mapping. *Electroencephalography and Clinical Neurophysiology, 72*, 184–187.

Pillon, B., Dubois, B., Bonnet, A. M., Esteguy, M., Guimaraes, J., Vigouret, J. M., et al. (1989). Cognitive slowing in Parkinson's disease fails to respond to levodopa treatment: The 15-objects test. *Neurology, 39*, 762–768.

Pliszka, S. R., Liotti, M., & Woldorff, M. G. (2000). Inhibitory control in children with attention-deficit/hyperactivity disorder: Event-related potentials identify the processing component and timing of an impaired right-frontal response-inhibition mechanism. *Biological Psychiatry, 48*, 238–246.

Prasher, D., & Findley, L. (1991). Dopaminergic induced changes in cognitive and motor processing in Parkinson's disease: An electrophysiological investigation. *Journal of Neurology, Neurosurgery, and Psychiatry, 54*, 603–609.

Pulvermuller, F., Lutzenberger, W., Muller, V., Mohr, B., Dichgans, J., & Birbaumer, N. (1996). P3 and contingent negative variation in Parkinson's disease. *Electroencephalography and Clinical Neurophysiology, 98*, 456–467.

Raskin, S. A., Borod, J. C., & Tweedy, J. R. (1992). Set-shifting and spatial orientation in patients with Parkinson's disease. *Journal of Clinical and Experimental Neuropsychology, 14*, 801–821.

Ritter, W., Simson, R., Vaughan, H. G. J., & Macht, M. (1982). Manipulation of event-related potential manifestations of information processing stages. *Science, 26*, 909–911.

Rumbach, L., Tranchant, C., Viel, J. F., & Warter, J. M. (1993). Event-related potentials in Parkinson's disease: A 12-month follow-up study. *Journal of the Neurological Sciences, 116*, 148–151.

Sohn, Y. H., Kim, G. W., Huh, K., & Kim, J. S. (1998). Dopaminergic influences on the P300 abnormality in Parkinson's disease. *Journal of the Neurological Sciences, 158*, 83–87.

Stanzione, P., Fattapposta, F., Giunti, P., D'Alessio, C., Tagliati, M., Affricano, C., et al. (1991). P300 variations in parkinsonian patients before and during dopaminergic monotherapy: a suggested dopamine component in P300. *Electroencephalography and Clinical Neurophysiology, 80*, 446–453.

Starkstein, S. E., & Robinson, R. G. (1997). Mechanism of disinhibition after brain lesions. *Journal of Nervous and Mental Disease, 185*, 108–114.

Stern, Y., Mayeux, R., & Cote, L. (1984). Reaction time and vigilance in Parkinson's disease. Possible role of altered norepinephrine metabolism. *Archives of Neurology, 41*, 1086–1089.

Strik, W. K., Fallgatter, A. J., Brandeis, D., & Pascual-Marqui, R. D. (1998). Three-dimensional tomography of event-related potentials during response inhibition: Evidence for phasic frontal lobe activation. *Electroencephalography and Clinical Neurophysiology, 108*, 406–413.

Tachibana, H., Aragane, K., Miyata, Y., & Sugita, M. (1997). Electrophysiological analysis of cognitive slowing in Parkinson's disease. *Journal of the Neurological Sciences, 149*, 47–56.

Tachibana, H., Toda, L., & Sugita, M. (1992). Actively and passively evoked P3 latency of event-related potentials in Parkinson's disease. *Journal of the Neurological Sciences, 111*, 134–142.

Taylor, S. F., Kornblum, S., Minoshima, S., Oliver, L. M., & Koeppe, R. A. (1994). Changes in medial cortical blood flow with a stimulus-response compatibility task. *Neuropsychologia, 32*, 249–255.

Toda, K., Tachibana, H., Sugita, M., & Konishi, K. (1993). P300 and reaction time in Parkinson's disease. *Journal of Geriatric Psychiatry and Neurology, 6*, 131–136.

Tsuchiya, H., Yamaguchi, S., & Kobayashi, S. (2000). Impaired novelty detection and frontal lobe dysfunction in Parkinson's disease. *Neuropsychologia, 38*, 645–654.

Tucker, D. M. (1993). Spatial sampling of head electrical fields: the geodesic sensor net. *Electroencephalography and Clinical Neurophysiology., 87*, 154–163.

Weisbrod, M., Kiefer, M., Marzinzik, F., & Spitzer, M. (2000). Executive control is disturbed in schizophrenia: evidence from event- related potentials in a Go/NoGo task. *Biological Psychiatry, 47*, 51–60.

Effects of Aging on Regional Cerebral Blood Flow Assessed By Using Technetium Tc 99m Hexamethylpropyleneamine Oxime Single-Photon Emission Tomography with 3D Stereotactic Surface Projection Analysis

Kazuo Takahashi, Shuhei Yamaguchi, Shotai Kobayashi, and Yasushi Yamamoto

OBJECTIVES: **Although many previous reports have described age-related changes in regional cerebral blood flow (rCBF), none has used 3D stereotactic surface projection (3D-SSP) analysis, which is able to detect subtle and significant changes in rCBF.**

METHODS: **The subjects were 31 healthy volunteers (16 men and 15 women; 50–79 years of age) without abnormal MR imaging and MR angiographic findings, cognitive impairment, or depression. For each subject, rCBF was evaluated by using technetium Tc 99m-radiolabeled hexamethylpropyleneamine oxime single-photon emission CT. Maps of rCBF were compared among different age groups (50–59, 60–69, and 70–79 years of age) by using 3D-SSP. The mean *z* score for each gyrus was calculated for each age group by using a recently developed stereotactic extraction estimation method.**

RESULTS: **Significant age-related reductions in rCBF were seen in the bilateral cingulate gyri, left inferior gyrus, bilateral medial frontal gyri, left subcallosal gyrus, and left superior temporal gyrus. Extensive and constant reduction in rCBF occurred with increasing age in the bilateral anterior cingulate gyri, and the mean *z* score for this region was the highest among all the regions examined.**

CONCLUSION: **The 3D-SSP analysis revealed that the greatest reduction in rCBF occurred within the bilateral anterior cingulate gyri in normal middle-aged and older subjects.**

Many previous reports have described age-related changes in regional cerebral blood flow (rCBF) (1–9). In the cingulate gyrus, frontal lobe, parietal lobe, and temporal lobe, rCBF has been reported to diminish with age in normal subjects, even in relatively young subjects (20–40 years of age). Nevertheless, there is at least one report that the reduction in rCBF was negligible in subjects >40 years of age (1). Although several reports describe the anterior cingulate as the main site within which rCBF is reduced with normal aging (2–5), other studies failed to demonstrate any reduction in rCBF in this area (6, 7). These discrepancies may be attributable to differences in the criteria used to select subjects and the diversity of the image analysis methods. We strictly selected healthy middle-aged and older subjects who had undergone 1.5T MR imaging and MR angiography (MRA) and who had no brain lesion or major vessel stenosis, both of which are factors that influence rCBF. This is in contrast to many previous studies in which subjects were not assessed by using MR imaging (1, 5–8). Moreover, in no studies of rCBF has MRA been used to evaluate major vessels. We also assessed the mental status of all subjects.

Some authors have evaluated the relationship between rCBF and normal aging by using statistic parametric mapping (SPM) (2, 3, 5), but, to our knowledge, no one has used 3D stereotactic surface projection (3D-SSP) analysis. 3D-SSP analysis is a fully automated, user-independent method for data extraction that allows (1) pixel-by-pixel analysis of cerebral perfusion, (2) anatomic normalization of individual single photon emission CT (SPECT) data to the standard brain, and (3) comparison of regional voxel data between 2 different groups. 3D-SSP anal-

Received October 28, 2004; accepted after revision March 2, 2005.

From the Departments of Neurology, Hematology, and Rheumatology, School of Medicine, Shimane University (K.T., S.Y., S.K.), and the Radiological Center, Shimane University Hospital (Y.Y.), Shimane, Japan.

Address correspondence to Kazuo Takahashi, MD, Department of Neurology, Hematology and Rheumatology, Shimane University School of Medicine, 89-1 Enyacho, Izumo, Shimane 693-8501, Japan.

TABLE 1: Mean age, verbal intelligence, and SDS in each age group

Age group (y)	50–59	60–69	70–79
Number (M:F)	10 (4:6)	12 (7:5)	9 (5:4)
Mean age (y)	55.2 ± 3.0	63.8 ± 2.9	73.2 ± 2.4
Okabe's Scale, total	48.9 ± 3.0	47.0 ± 5.7	45.4 ± 6.9
Information	18.4 ± 1.6	17.5 ± 1.7	16.4 ± 1.9
Mental control	14.5 ± 1.6	12.4 ± 3.3	12.8 ± 2.9
Digit span	9.0 ± 1.6	8.9 ± 1.5	9.2 ± 0.7
Associate learning	7.0 ± 3.9	8.2 ± 3.6	7.0 ± 3.6
SDS	30.8 ± 5.9	28.9 ± 4.3	29.7 ± 5.7

Note.—Okabe Scale indicates Okabe's Simplified Intelligence Scale (60-point scale); SDS, Zung Self-Rating Depression Scale (80-point scale).

ysis provides a reliable and objective evaluation of the severity, extent, and localization of cortical perfusion abnormalities in 2 groups (10–14). The difference between 3D-SSP analysis and SPM is the intrinsic performance of the algorithms used by each method, including image-matching fusion, pixel interpolation, and axial rotation. The 3D-SSP algorithm uses prior knowledge of brain anatomy and deforms the shape of the brain along the direction of cortical projection fibers (15). This process is thought to be particularly advantageous for standardizing atrophied brains (15). Because brain atrophy occurs with aging in healthy subjects, we believe that 3D-SSP is an excellent method for evaluating changes in rCBF owing to normal aging.

Materials and Methods

Subjects

Thirty-one healthy subjects (15 men and 16 women; 10 in their 50s, 12 in their 60s, and 9 in their 70s) were recruited from among persons who received screening for brain health (brain check-up) at Shimane Institute of Health Science for the purpose of making a normal control data base for 3D-SSP analysis by using the following criteria: (1) 50–79 years of age; (2) physically healthy and free of psychiatric disorders; (3) no history of stroke; (4) no findings of brain atrophy, asymptomatic white matter lesion, or stroke lesion by T1, T2, fluid-attenuated inversion recovery, or T2-weighted MR imaging (1.5-Tesla; Siemens Symphony, Munich, Germany); (5) no findings of stenosis of major vessels or aneurysm by head MR angiography; (6) score of >35 points on the Okabe Simplified Intelligence Scale (Okabe Score) (16); and (7) score of <40 points on the Zung Self-Rating Depression Scale (SDS) (17). The Okabe test is a modified and simplified version of the Wechsler Memory Scale and consists of 4 subscales: information, mental control, digit span, and associative learning. The full scores on these 4 subscales total 60 points. The classification criteria are 20–29 points, mild dementia (or notable mental aging); 10–19 points, moderate dementia; <10 points, severe dementia (16). The 20 items of the SDS test are scored on a standard 4-point scale (1–4) for each item, with potential results ranging from 20 to 80. A score of >40 (raw score) is considered to be depressive state. The results of the Okabe test and SDS are shown in Table 1.

SPECT Imaging

Regional CBF images were obtained by SPECT by using technetium Tc 99m-hexamethylpropyleneamine oxime (HM-PAO). All subjects were studied in the supine resting position with closed eyes in a silent room from approximately 16:00 to 17:00 hours. The SPECT images were acquired on a PRISM IRIX (Marconi, Cleveland, OH), 3-headed SPECT camera with ultrahigh-resolution fan-beam collimators. The data acquisition parameters were 128 × 128 matrices (2.33-mm pixel

TABLE 2: Mean *z* score for each region between each age generation

	Relative Decrease of rCBF, Age (y)		
	60–69 vs 50–59	70–79 vs 60–69	70–79 vs 50–59
Superior frontal gyrus			
L	0.80 ± 0.51	1.59 ± 0.45	0.64 ± 0.46
R	0.73 ± 0.59	1.49 ± 0.35	0.67 ± 0.41
Middle frontal gyrus			
L	0.60 ± 0.43	1.37 ± 0.32	0.99 ± 0.58
R	0.66 ± 0.53	1.49 ± 0.44	0.66 ± 0.48
Inferior frontal gyrus			
L	0.71 ± 0.53	1.97 ± 0.57	1.53 ± 0.72
R	0.53 ± 0.37	1.39 ± 0.38	1.14 ± 0.64
Medial frontal gyrus			
L	1.38 ± 0.84	1.62 ± 0.58	1.33 ± 0.99
R	1.37 ± 0.94	1.30 ± 0.16	1.37 ± 0.97
Subcallosal gyrus			
L	1.30 ± 1.04	2.08 ± 0.54	1.73 ± 0.59
R	1.47 ± 1.11	1.22 ± 0.13	0.83 ± 0.37
Superior parietal lobule			
L	0.24 ± 0.17	1.27 ± 0.17	0
R	0	0	0
Inferior parietal lobule			
L	0.12 ± 0.12	1.50 ± 0.35	0.63 ± 0.48
R	0.63 ± 0.55	1.12 ± 0.06	0.56 ± 0.40
Superior temporal gyrus			
L	1.19 ± 0.72	1.61 ± 0.43	1.97 ± 0.82
R	1.03 ± 0.69	1.37 ± 0.24	1.33 ± 0.96
Middle temporal gyrus			
L	0.95 ± 0.74	1.44 ± 0.34	1.13 ± 0.72
R	0.42 ± 0.28	1.47 ± 0.27	0.82 ± 0.69
Inferior temporal gyrus			
L	0.76 ± 0.42	1.56 ± 0.47	0.82 ± 0.45
R	0.92 ± 0.66	1.27 ± 0.19	1.20 ± 0.65
Cuneus			
L	1.29 ± 0.92	0	0.71 ± 0.63
R	0.93 ± 0.74	1.08 ± 0.04	0.36 ± 0.28
Lingual gyrus			
L	0.70 ± 0.58	0	0.84 ± 0.55
R	0.49 ± 0.47	1.39 ± 0.25	0.70 ± 0.38
Anterior cingulate gyrus			
L	1.55 ± 0.61	1.87 ± 0.59	2.51 ± 0.81
R	1.79 ± 0.73	2.02 ± 0.60	2.89 ± 0.99
Posterior cingulate gyrus			
L	1.31 ± 1.11	1.40 ± 0.27	1.42 ± 0.70
R	1.20 ± 0.81	1.56 ± 0.26	1.51 ± 0.48
Parahippocampal gyrus			
L	0.44 ± 0.24	1.43 ± 0.29	0.97 ± 0.52
R	1.26 ± 0.65	1.73 ± 0.59	0.78 ± 0.45
Superior occipital gyrus			
L	0.06 ± 0	0	0
R	0.76 ± 0.28	0	0.29 ± 0.15
Middle occipital gyrus			
L	0.47 ± 0.44	0	0.45 ± 0.19
R	0.68 ± 0.39	0	0.56 ± 0.45
Inferior occipital gyrus			
L	0	0	0
R	0.05 ± 0	0	0

size), 5° per step, 72 views, 30 seconds per view, 2× zoom, and a 140-keV (± 7.5) energy window. The subjects were injected with 370 MBq of technetium Tc 99m-HMPAO in the antecubital vein of the right arm, and the dynamic data acquisition for the Patlak method was performed. Subjects were then injected with 370 MBq technetium Tc 99m-HMPAO again for SPECT acquisition. Reconstruction was performed by filtered back projection by using a Butterworth filter (cut-off frequency, 0.25 cycle/pixel) and ramp filters with attenuation correction by using the Chang 8-order method (μ = 0.09/cm).

3D-SSP Analysis

Because the size and form of each individual's head is different, it is difficult to compare the SPECT findings between 2 different groups reliably and objectively; however, 3D-SSP analysis enables us to make statistical comparisons easily. Analysis by 3D-SSP anatomically normalizes the individual SPECT data to the standard brain and compares the regional voxel data between 2 different groups (10–14). This procedure was performed by the interface software iSSP (version 3.5, Nihon Medi-Physics Corporation, Nishinomiya, Japan).

First, stereotactic anatomic standardization was performed. Rotational correction and centering in 3 dimensions of the SPECT dataset were conducted, followed by realignment to the anterior commissureposterior commissure line. The anterior commissure–posterior commissure line was estimated by iterative matching between the individual images and the template from the Talairach and Tournoux atlas (18) by using mutual information. Differences in size between the individual brain and standard template were eliminated by linear scaling. Regional anatomic differences between the individual and the standard atlas brain were thus minimized by automated nonlinear warping.

In the data extraction step, >16,000 surface pixels covering the lateral and medial surfaces of both hemispheres were predetermined with stereotactic coordinates. The peak cortical activity perpendicular to these pixels was projected onto the surface pixels. The pixel values of an individual's image set were normalized to the mean global CBF before the analysis. Therefore, each brain was stereotactically transformed into a standard surface image format, which enabled us to compare the resultant cortical projections between the 2 groups. To demonstrate the differences in the rCBF patterns, 2-sample *t* test values were calculated on a pixel-by-pixel basis between 2 groups and then transformed to *z* values by a probability integral transformation.

Differences in the rCBF Patterns between Age Groups

By using the SPECT data of the subjects, we performed 3D-SSP analysis to compare age groups. To quantify perfusion deficits, pixel-by-pixel *z* scores were used. *z* scores ([mean of normalized pixel value of one age group] − [mean normalized pixel value of other age group])/[SD of one age group]) were calculated for each surface pixel. A positive *z* score represents a reduced rCBF in the one group relative to the other group. We used a *z* score of 2 as the cutoff value. To assess the rCBF reduction quantitatively, the mean *z* scores for the each lobe and gyrus level classification was calculated by the recent developed stereotactic extraction estimation (SEE) method (19). Mean *z* score for each gyrus was automatically measured (average *z* value of the coordinates with a *z* value that exceeds 0 of the threshold value).

This study was approved by the local ethics committee of Shimane University Hospital. Written informed consent was obtained from all subjects.

Results

Statistical maps (Fig 1) showed relative reduction of rCBF between each age group (*z* score ≦2). The extensive and constant reduction of the rCBF was significantly observed in the bilateral anterior cingulate gyri between each age group. The age-related reduction of rCBF in the left superior temporal gyrus and left subcallosal gyrus was also constantly observed between each age group (Fig 1*A–C*). In addition, there were decreases in the rCBF of the bilateral medial frontal gyri and bilateral posterior cingulate gyri in the 60–69-year-old group and the 70–79-year-old group compared with those in the 50–59-year-old group (Fig 1*A, -C*). The rCBF of the left inferior frontal gyrus in the 70–79-year-old group was significantly lower than that of the 50–59-year-old group or the 60–69-year-old group (Fig 1*B, -C*). There were also decreases in the rCBF of right superior and inferior temporal gyrus in the 70–79-year-old group compared with those in the 50–59-year-old group (Fig 1*C*).

Table 2 shows mean *z* scores for the each lobe and gyrus level classification between each age group. Mean *z* score of bilateral anterior cingulate gyri was relatively higher than other lobe and gyrus. The *z* scores for all the significant reductions of rCBF shown above were within 4.5.

Discussion

Although this study revealed age-related reductions in rCBF at several sites, the most marked reduction in rCBF was in the anterior cingulate gyrus, particularly between subjects in their 50s and those in their 70s. Several authors have identified an association between aging and reduced rCBF in the anterior cingulate gyrus. Waldermar et al (8) evaluated rCBF in 53 healthy subjects (21–83 years of age) by using technetium Tc 99m-radiolabeled-HMPAO SPECT and found that rCBF in the upper frontal cortex, superior frontal gyrus, cingulate gyrus, and upper parietal cortex decreased with increasing age. Some studies of age-related changes of rCBF used ethyl cysteinate dimer SPECT. Nakano et al (2) performed rCBF measurements by using the Patlak Plot method in 53 normal volunteers (18–87 years of age). Their results, analyzed by SPM, revealed significant age-related decreases in rCBF in the limbic area and in the associative cortices, such as the prefrontal cortices, anterior cingulate gyri, and insular cortices or bilateral temporal poles. Van Laere et al (3) measured rCBF in 89 healthy volunteers (20–81 years of age) and reported that rCBF declined with age in the anterior cingulate gyrus, the bilateral basal ganglia, and the left prefrontal, left lateral frontal, left superior temporal, and insular cortices. Tanaka et al (4) also reported significant age-related decreases in rCBF in the anterior and posterior cingulate cortex, superior prefrontal and parietal cortex, striatum, and hippocampus in 48 normal subjects (22–95 years of age). Martin et al (5) used positron-emission tomography to demonstrate age-related decreases in rCBF in the cingulate, parahippocampal, superior temporal, medial frontal, and posterior cortices bilaterally and

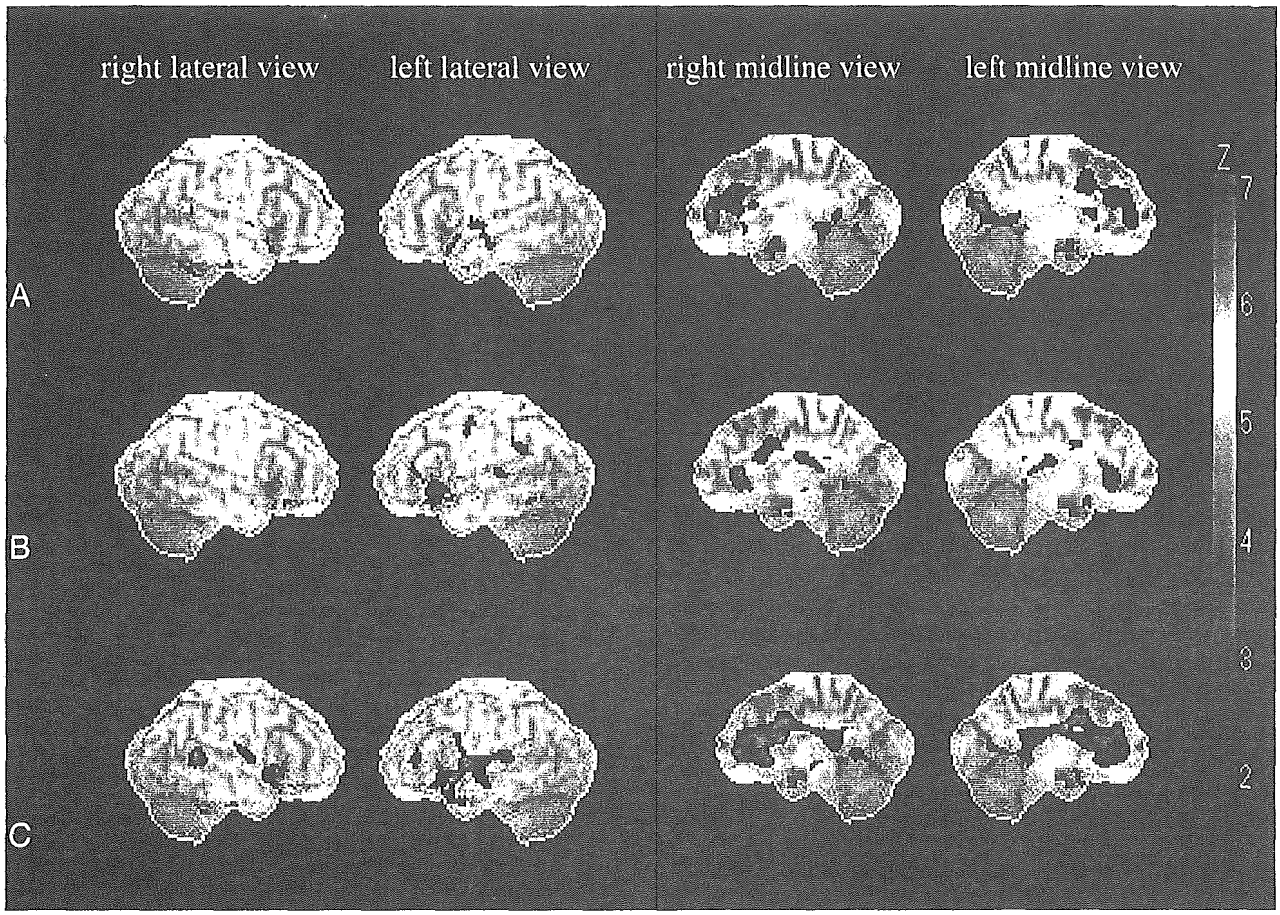

FIG 1. Statistical maps analyzed by 3D SSP. The color of the outer counter corresponds to a *Z* score of 7.

A, Relative decreases of rCBF (*z* score ≦2) in subjects 60–69 years of age compared with rCBF in subjects 50–59 years of age. The most extensive reduction in rCBF was observed in the right anterior cingulate gyrus. There were also decreases in rCBF in the left anterior cingulate gyrus, bilateral posterior cingulate gyri, bilateral medial frontal gyri, bilateral subcallosal gyri, left superior temporal gyrus, and left cuneus.

B, Relative decreases of rCBF (*z* score ≦2) in subjects 70–79 years of age compared with rCBF in subjects 60–69 years of age. The most extensive reduction in rCBF was observed in the bilateral anterior cingulate gyri. There were also decreases in rCBF in the left inferior frontal gyrus, left subcallosal gyrus, left supramarginal gyrus, and left superior temporal gyrus.

C, Relative decreases of rCBFs (*z* score ≦2) in subjects 70–79 years of age compared with rCBF in subjects 50–59 years of age. The most extensive reduction in rCBF was observed in the bilateral anterior cingulate gyri. There were also decreases in rCBF in the left inferior frontal gyrus, left subcallosal gyrus, left supramarginal gyrus, and left superior temporal gyrus.

in the left insular and left posterior prefrontal cortices in 30 normal subjects (30–85 years of age).

There have been some contradictory results related to the association between aging and a reduction in rCBF in the anterior cingulate gyrus. Pagani et al (6) assessed rCBF in 50 healthy subjects (31–78 years of age) by using HMPAO-SPECT, and found a significant decrease in rCBF with increasing age in the temporocingulate cortex, but not in the anterior cingulate gyrus. Mozley et al (1) evaluated rCBF in 44 healthy subjects (19–73 years of age) by using HMPAO-SPECT and found age-related decreases in rCBF in many parts of the gray matter, including the anterior cingulate gyrus; however, most of the age-related changes were observed in young adults, and the reduction in rCBF was negligible after middle age. Krausz et al (7) compared rCBF in younger healthy subjects (26–47 years of age) and older healthy subjects (47–71 years of age) by using HMPAO-SPECT. Their analysis was performed by applying 3 preformed templates, each of which contained delineated regions of interest, to 3 transaxial brain sections at approximately 4, 6, and 7 cm above the orbitomeatal line. They found no age-related change in rCBF after normalizing the data to rCBF in the cerebellum, whereas significantly increased uptake ratios were observed in the cingulate cortex on the basis of the data normalized to the whole section. Jones et al (9) compared rCBF in healthy subjects 50–72 years of age with those 72–92 years of age and found no significant age-related differences in whole-brain HMPAO uptake, except in the lateral ventricular regions. The results of the study by Krausz et al (7) are exceptional among the studies discussed here: these authors found that rCBF in the anterior cingulate gyrus was reduced with aging in normal subjects, including subjects between 20 and 40 years of age, but that the reduction in rCBF was unremarkable among subjects >50 years of age. In the present study, the age-related reduction in rCBF was extensive in the

anterior cingulate in normal subjects 50–79 years of age. All *z* scores for reductions in rCBF were within 4.5 in the present study, which suggested that the degree of reduction in rCBF was not severe, but significant. To our knowledge, there have been no reports of the relationship between normal aging and rCBF based on the use of 3D-SSP HMPAO SPECT. In light of the fact that 3D-SSP analysis allows pixel-by-pixel analysis of cerebral perfusion and provides a reliable and objective evaluation of the severity and localization of differences in cortical perfusion, this method makes it possible to detect subtle changes in rCBF with aging that might not be detectable by using other methods. Another advantage of 3D-SSP HMPAO SPECT over other methods is the superior mean of standardization of atrophied brains (15).

Some authors reported that patients with pain or psychiatric disorders following anterior cingulotomy exhibited little cognitive impairment (20, 21). The anterior cingulate gyrus is part of the largest formation of the limbic system and is thought to be associated with emotion, attention (22), memory, initiation, motivation, goal-directed behaviors (23), and working memory (24). We believe that reduced rCBF in the anterior cingulate gyrus may not affect general cognition but might cause subtle cognitive impairment with aging.

In conclusion, we observed an age-related reduction in rCBF mainly in the bilateral cingulate gyri, left inferior gyrus, bilateral medial frontal gyri, left subcallosal gyrus, and left superior temporal gyrus in healthy subjects. The greatest reduction in rCBF occurred within the bilateral anterior cingulate gyri.

Acknowledgments

The study was partly supported by a research grant from Nihon Medi-Physics.

References

1. Mozley PD, Sadek AM, Alavi A, et al. **Effects of aging on the cerebral distribution of technetium-99m hexamethylpropylene amine oxime in healthy humans.** *Eur J Nucl Med* 1997;24:754–761
2. Nakano S, Asada T, Matsuda H, et al. **Effects of healthy aging on the regional cerebral blood flow measurements using ^{99m}Tc-ECD SPECT assessed with statistical parametric mapping.** *Nippon Ronen Igakkai Zasshi* 2000;37:49–55
3. Van Laere K, Versijpt J, Audenaert K, et al. **^{99m}Tc-ECD brain perfusion SPET: variability, asymmetry and effects of age and gender in healthy adults.** *Eur J Nucl Med* 2001;28:873–887
4. Tanaka F, Vines D, Tsuchida T, et al. **Normal patterns on ^{99m}Tc-ECD brain SPECT scans in adults.** *J Nucl Med* 2000;41:1456–1464
5. Martin AJ, Friston KJ, Colebatch JG, Frackowiak RSJ. **Decreases in regional cerebral blood flow with normal aging.** *J Cereb Blood Flow Metab* 1991;11:684–689
6. Pagani M, Salmaso D, Jonsson C, et al. **Regional cerebral blood flow as assessed by principal component analysis and ^{99m}Tc-HMPAO SPET in healthy subjects at rest: normal distribution and effect of age and gender.** *Eur J Nucl Med* 2002;29:67–75
7. Krausz Y, Bonne O, Gorfine M, et al. **Age-related changes in brain perfusion of normal subjects detected by ^{99m}Tc-HMPAO SPECT.** *Neuroradiology* 1998;40:428–434
8. Waldemar G, Hasselbalch SG, Andersen AR, et al. **99mTc-d,l-HMAPO and SPECT of the brain in normal aging.** *J Cereb Blood Flow Metab* 1991;11:508–521
9. Jones K, Johnson KA, Becker JA, et al. **Use of singular value decomposition to characterize age and gender differences in SPECT cerebral perfusion.** *J Nucl Med* 1998;39:965–973
10. Minoshima S, Frey KA, Koeppe RA, et al. **A diagnostic approach in Alzheimer's disease using three-dimensional stereotactic surface projections of fluorine-18-FDG PET.** *J Nucl Med* 1995;36:1238–1248
11. Burdette JH, Minoshima S, Vander Borght T, et al. **Alzheimer disease: improved visual interpretation of PET images by using three-dimensional stereotaxic surface projections.** *Radiology* 1996;198:837–843
12. Honda N, Machida K, Matsumoto T, et al. **Three-dimensional stereotactic surface projection of brain perfusion SPECT improves diagnosis of Alzheimer's disease.** *Ann Nucl Med* 2003;17:641–648
13. Hanyu H, Shimuzu S, Tanaka Y, et al. **Cerebral blood flow patterns in Binswanger's disease: a SPECT study using three-dimensional stereotactic surface projections.** *J Neurol Sci* 2004;220:79–84
14. Kaneko K, Kuwabara Y, Sasaki M, et al. **Posterior cingulate hypoperfusion in Alzheimer's disease, senile dementia of Alzheimer type, and other dementias evaluated by three-dimensional stereotactic surface projections using Tc-99m HMPAO SPECT.** *Clin Nucl Med* 2004;29:362–366
15. Ishii K, Willoch F, Minoshima S, et al. **Statistical brain mapping of ^{18}F-FDG PET in Alzheimer's disease: validation of anatomic standardization for atrophied brains.** *J Nucl Med* 2001;42:548–557
16. Fukunisi I, Okabe S, Nakagawa T, Hosokawa K. **The assessment of intelligence function of aged chronic schizophrenia.** *Jpn J Psychiatry Neurol.* 1990;44:503–509
17. Zung WW. **A self-rating depression scale.** *Arch Gen Psychiatry* 1965;12:63–70
18. Talairach J, Tournoux P. ***Co-planar stereotactic atlas of the human brain.*** New York: Thieme; 1988
19. Mizumura S, Kumita S, Cho K, et al. **Development of quantitative analysis method for stereotactic brain image: assessment of reduced accumulation in extent and severity using anatomical segmentation.** *Ann Nucl Med* 2003;17:289–295
20. Kim CH, Chang JW, Koo MS, et al. **Anterior cingulotomy for refractory obsessive-compulsive disorder.** *Acta Psychiatr Scand* 2003;107:283–290
21. Dougherty DD, Baer L, Cosgrove GR, et al. **Prospective long-term follow-up of 44 patients who received cingulotomy for treatment-refractory obsessive-compulsive disorder.** *Am J Psychiatry* 2002;159:269–275
22. Cohen RA, Paul R, Zawacki TM, et al. **Emotional and personality changes following cingulotomy.** *Emotion* 2001;1:38–50
23. Devinsky O, Morrell MJ, Vogt BA. **Contributions of anterior cingulate cortex to behaviour.** *Brain* 1995;118:279–306
24. Osaka N, Osaka M, Kondo H, et al. **The neural basis of executive function in working memory: an fMRI study based on individual differences.** *Neuroimage* 2004;21:623–631

Journal of Neuroscience Research 81:342–348 (2005)

Mini-Review

Immortalized Human Microglial Cell Line: Phenotypic Expression

Atsushi Nagai,[1] Seiji Mishima,[2] Yuri Ishida,[1] Hiroto Ishikura,[3] Takayuki Harada,[4] Shotai Kobayashi,[1] and Seung U. Kim[5,6]*

[1]Department of Neurology, Shimane University School of Medicine, Izumo, Japan
[2]Department of Blood Transfusion, Shimane University School of Medicine, Izumo, Japan
[3]Department of Clinical Oncology, Shimane University School of Medicine, Izumo, Japan
[4]Department of Pathology, Shimane University School of Medicine, Izumo, Japan
[5]Department of Neurology, University of British Columbia, Vancouver, British Columbia, Canada
[6]Brain Disease Research Center, Ajou University School of Medicine, Suwon, Korea

Microglia are a major neuroglial component of the CNS, playing an important role as resident immunocompetent and phagocytic cells in the CNS in the event of injury and disease. To understand the role of microglia in the CNS in health and diseases, we have recently established an immortalized clonal cell line of human microglia, HMO6, from human embryonic telencephalon tissue by using a retroviral vector encoding v-myc. This immortalized microglia HMO6 cell line exhibits cell-type-specific antigens for microglia, including CD11b (Mac-1), CD68, CD86 (B7-2), HLA-ABC, HLA-DR, and RCA-1 lectin, and actively phagocytoses latex beads.

Key words: HMO6; microglial cell line; phenotype

MICROGLIA AS IMMUNOCOMPETENT CELLS OF THE CNS

Microglia as the resident phagoyitic cells of the central nervous system (CNS) were first described and named by del Rio Hortega (1932), and make up 5–12% of the neuron-glia cell population of the CNS (Perry and Gordon, 1991). Although origin and turnover of microglia in adult brain have remained enigmatic, a widely accepted theory holds that monocyte precursor cells populate the brain during the early CNS development and give rise to microglia.

In health, expression of proteins with immunologic properties in the CNS cells is low, because the CNS is shielded by the blood–brain barrier (BBB), which restricts entry of plasma proteins and immune cells into the CNS parenchyma. After injuries or infection within the CNS, such as trauma, stroke, Alzheimer's disease, AIDS dementia, and multiple sclerosis, the normally quiescent microglia are transformed into highly activated cells expressing macrophage-related antigens, such as MHC-I, MHC-II, complement receptor 3, and costimulatory molecules, and migrate to the site of injury, proliferate, and phagocytose both microorganisms and host tissues (Flaris et al., 1993; McGeer et al., 1993; Kreutzberg, 1996; Shrikant and Benveniste, 1996). Activated microglia release cytokines and chemokines, such as interleukin (IL)-1β, IL-6, tumor necrosis factor (TNF)-α and MIP-1α, which are involved in development of inflammation and in recruitment of inflammatory cells to the focal brain lesions. Microglia are also known as the source of neurotrophic factors, such as glial cell line-derived neurotrophic factor (GDNF) and brain-derived neurotrophic factor (BDNF), in the CNS. In this situation, serial expressions of surface antigens trigger events leading to immune responses and may play a key role in initiating inflammation in the CNS.

To understand the role of microglia in the CNS in health and diseases, we have previously established an immortalized clonal cell line of human microglia, HMO6, from human embryonic telencephalon tissue by using a retroviral vector encoding v-myc (Nagai et al., 2001b). In the following sections, the phenotype of human microglia isolated from fetal brain and HMO6 human microglia cell line as investigated by immunocytochemistry and fluorescence-activated cell sorting (FACS) analyses is described.

Contract grant sponsor: Mitsubishi Pharma Research Foundation; Contract grant sponsor: Canadian Myelin Research Initiative; Contract grant sponsor: KOSEF/BDRC Ajou University.

*Correspondence to: Seung U. Kim, MD, PhD, Department of Neurology, UBC Hospital, University of British Columbia, 2211 Wesbrook Mall, Vancouver, British Columbia, V6T 2B5 Canada.
E-mail: sukim@interchange.ubc.ca

Received 29 July 2004; Accepted 10 August 2004

Published online 14 June 2005 in Wiley InterScience (www.interscience.wiley.com). DOI: 10.1002/jnr.20478

TABLE I. Established Microglial Cells Lines

Clone	Origin	Immortalization method	Year	Authors
	Mouse	v-raf/v-myc Oncogenes	1990	Blasi et al.
	Mouse		1993	Corradin et al.
	Mouse		1994	Briers et al.
EOC	Mouse		1995	Walker et al.
MG5	Mouse	p53-Deficient mice	1997	Ohsawa et al.
RBM129	Rat	SV40 Large T antigen	1992	Hosaka et al.
	Rat	SV40 Large T antigen	1995	McLaurin et al.
Ra2	Rat		1998	Sawada et al.
HAP1	Rat	Spontaneous	2001	Cheepsunthorn et al.
CHME	Human	SV40 Large T antigen	1995	Janabi et al.
HMO6	Human	v-myc Oncogene	2001	Nagai et al.

GENERATION OF IMMORTALIZED HUMAN MICROGLIA CELL LINES

In the past, several mouse and rat microglia cell lines have been produced to obtain sufficient numbers of microglial cells to study detailed cellular and molecular properties of the cell type (Blasi et al., 1990; Hosaka et al., 1992; Corradin et al., 1993; Briers et al., 1994; McLaurin et al., 1995; Walker et al., 1995; Ohsawa et al., 1997; Sawada et al., 1998; Cheepsunthorn et al., 2001; Table I). As for human microglail cell lines, there was a single report of a human microglial cell line (Janabi et al., 1995), but the cell line expresses only limited number of microglia-specific antigens and does not qualify as an authentic microglia cell line. The HMO6 immortalized clonal cell line of human microglia was generated from a primary culture of fetal human cerebrum. Primary fetal human microglial cells were infected with the replication-incompetent mouse retrovirus PASK1 carrying pLNXvmyc vector to produce immortalized microglial cell lines. This HMO6 cell line exhibits cell-type-specific antigens for microglia, including CD11b (Mac-1), CD68, CD86 (B7-2), HLA-ABC, HLA-DR, and RCA-1 lectin, and actively phagocytoses latex beads. HMO6 cells, as in primary human microglia, show phenotypic expression of cytokines IL-1β, IL-6, IL-8, IL-10, IL-12, IL-15, and TNF-α. In addition HMO6 cells express chemokines MIP-α1, MIP-1β, and MCP (Nagai et al., 2001b).

Phenotypic expression and in vivo behavior of one of these human cell lines, HMO6, is dealt with in the present study. Because microglia are easily activated in response to changes in culture conditions, stable conditions of human microglial cell lines will be needed to examine the phenotype and biology of microglia.

PHENOTYPE EXPRESSION OF PRIMARY HUMAN MICROGLIA AND HMO6 HUMAN MICROGLIAL CELL LINE

Primary human microglial cell cultures were established from embryonic human brains of 12–15 weeks' gestation, as described previously (Satoh and Kim, 1994; Nagai et al., 2001a). Permission to use embryonic tissues

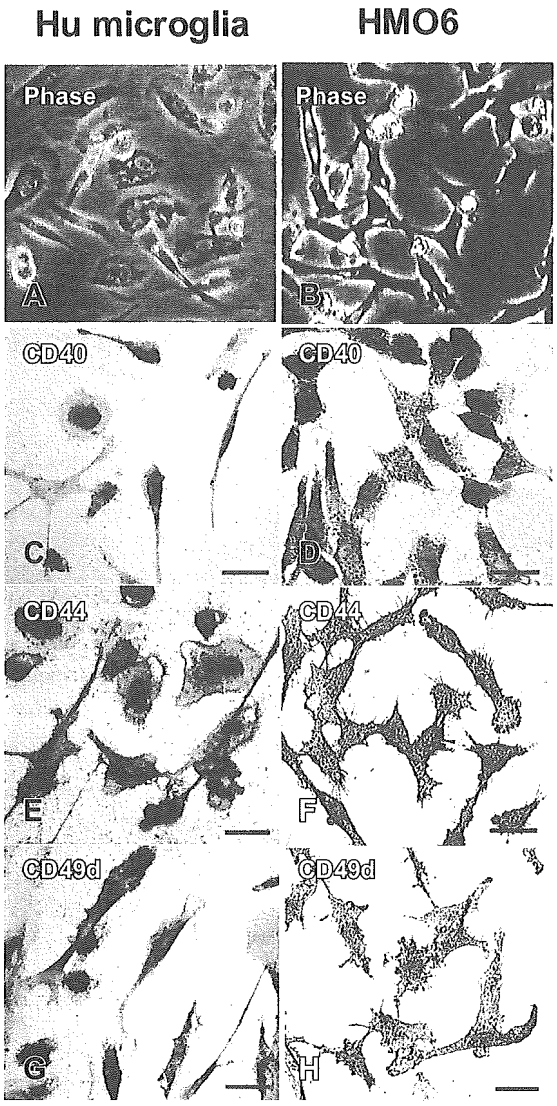

Fig. 1. Morphology and properties of human microglia (**A, C, E, G**) and HMO6 human microglial cell line (**B, D, F, H**).

was granted by the Clinical Screening Committee for Research Involving Human Subjects of the University of British Columbia. HMO6.N2, an immortalized microglial cell line, was established from a human primary microglial culture (Nagai et al., 2001b).

Immunostaining of primary human microglia revealed strong expression of cell surface antigens, including CD44, CD49d (VLA-4), and CD54 (ICAM-1). Expression of class I and class II major histocompatibilty antigens (HLA-ABC and HLA-DR) was detected in primary human microglia, and weak granular cell surface staining of both CD40 and CD99 was found on primary human microglia (Fig. 1A–C). Phenotypic expression of HMO6 immortalized human microglial cell line was similar to that of human primary microglia. Immunoreactivity for CD44, CD49d, and CD54 was also detected.

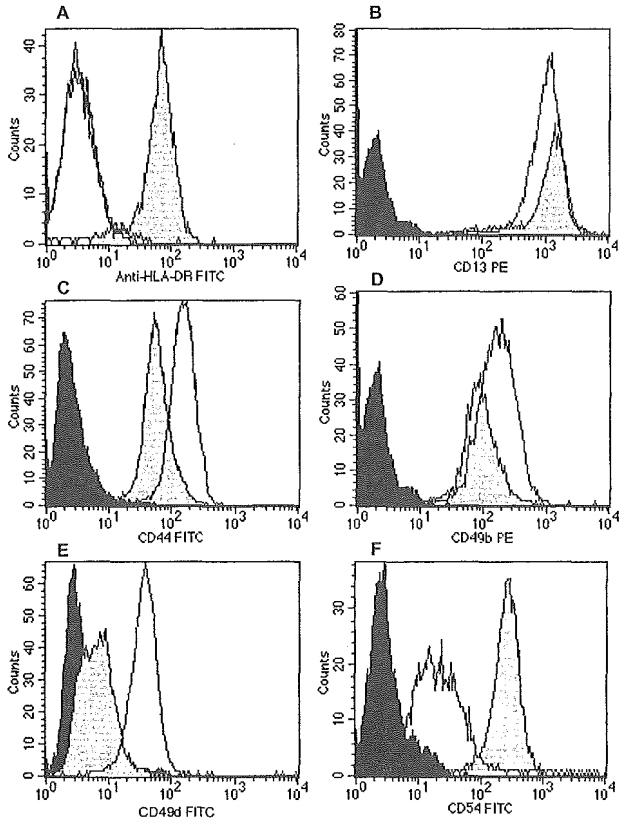

Fig. 2. Surface phenotype of HMO6 cells after treatment with IFN-γ (gray-colored), or after treatment with Aβ or LPS or no treatment (open) for 12 hrs. Black-colored = negative control.

However, no CD40 or CD99 was expressed by immunostaining (Fig. 1D–F). Expression of HLA-ABC and HLA-DR, MHC antigens, was readily induced by stimulation with 500 U of interferon (IFN)-γ for 12 hr in HMO6 cells. Nonspecific esterase, a cell-type-specific marker for phagocytic cells, was demonstrated both in primary human microglia and in HMO6 cells.

FLUORESCENCE-ACTIVATED CELL SORTING

The immunophenotype of immortalized human microglia cell line HMO6 cells was analyzed by fluorescence-activated cell sorting (FACS; Fig. 2, Table II) after 10–20 cell doublings. The antibodies utilized for FACS analysis are shown in Table II. Changes in the expression of surface antigens in HMO6 cells were also evaluated following treatment with IFN-γ, $A\beta_{1-42}$, and lipopolysaccharide (LPS). Analysis showed that CD13, a myeloid cell marker, was strongly expressed under nonstimulated as well as stimulate conditions. Expression of HLA-DR was negative under nonstimulated condition but was up-regulated after treatment with 500 U IFN-γ for 12 hr. CD54 expression was also up-regulated following treatment with IFN-γ. CD44, CD49b, CD49d, CD49e, and CD90 were stably expressed even after treatments (see Table II). However, expression level of CD49d (VLA-4), a ligand for VCAM-1, was decreased after IFN-γ treatment. Expression of CD11c was not induced in the present study.

ANTIGEN PRESENTATION

Microglia function as important immunoregulatory cells in the CNS; they express MHC-I, MHC-II, integrins, and Fc receptors and function as antigen-presenting cells (APCs) for T-cell activation. Immortalized human microglial cell line HMO6 has been shown to express Mac-1, complement receptor-3, MHC, and costimulatory factors B7-1 and B7-2, indicating that the cell line carries phenotypes characteristic of primary microglia (Nagai et al., 2001b). The further phenotype of HMO6 cells was determined in the present study. The cells did not express CD11c and HLA-DR under nonstimulated condition, suggesting that they have the characteristics of resting microglia. When responding to IFN-γ, they expressed HLA-DR, as seen in primary mouse microglial cells (Suzumura et al., 1987). They are negative for the monocytic markers CD4, CD14, CD11c, and myeloperoxidase.

RECEPTORS FOR SIGNALING MOLECULES

Microglia not only work as APCs but also respond to microenvironmental change as seen in in vitro studies after exposure to cytokines, chemokines, and other molecules such as ATP, ACh, and noradrenaline. Cell lines could be a useful tool for examining the exact effect of agents on the cells. Infection with HIV or stimulation with cytokines was reported to activate microglial cell lines through p42/p44 mitogen-activated protein kinase (MAPK), nuclear factor-κB (NFκB), and JAK-STAT pathways, which is a complex, multiparameter phenomenon that may involve many overlapping or distinct pathways depending on the stimulus (Bruce-Keller et al., 2001; Bright et al., 2004). Chemokines are important mediators of microglial cell recruitment to sites of injury, and, with in vitro study, monocyte chemoattractant protein 1 (MCP-1), macrophage inflammatory protein 1α (MIP-1α), MIP-1β, RANTES (regulated upon activation normal T cell expressed and secreted), IL-8, and interferon-γ inducible protein 10 (IP-10) induced migration and changes in the distribution of F-actin in the human cell line CHME (Cross, 1999). HMO6.N2 cells were revealed to retain purinergic receptors and showed rapid, transient increases in levels of intracellular Ca^{2+} in response to ATP (Nagai et al., 2001b).

CD40, an important receptor involved in cellular signaling and activation, plays a key role in inflammation (Karmann et al., 1995; Sempowski et al., 1997). Ligation of microglial CD40 leads to microglial activation as evidenced by TNF-α production and bystander neuronal injury (Tan et al., 1999). Although we detected weak expression of CD40 on human primary microglia under nonstimulated conditions, neither CD40 expression nor up-regulation was found in HMO.N2 cells with stimula-

TABLE II. Epitope Profile of HMO6 Analyzed by FACS*

Epitope	Source	Nonstimulated	IFN-γ	Aβ1–42	LPS
CD3	Immunotech				
CD4	Immunotech				
CD11a (LFA-1)	BD PharMingen				
CD11c	Immunotech				
CD13	Immunotech	+	+	+	+
CD14	Immunotech				
CD16	Immunotech				
CD31 (PECAM)	Santa Cruz				
CD33	Immunotech				
CD34	Immunotech				
CD36	Immunotech				
CD40	BD PharMingen				
CD44	BD PharMingen	+	+	+	+
CD45	Immunotech				
CD49b	BD PharMingen	+	+	+	+
CD49d (VLA-4)	BD PharMingen	+	±	+	+
CD49e	Immunotech	+	+	+	+
CD54 (ICAM-1)	BD PharMingen	±	+	±	±
CD79a	Immunotech				
CD80	Immunotech				
CD99	BD PharMingen				
CD117	Immunotech				
HLA-DR	Immunotech		+		
MPO	Immunotech				

*Analysis was evaluated on a scale ranging from − (negative), to ± (slightly positive), to + (positive). LFA-1, lymphocyte function-associated molecule-1; PECAM, platelat/endothelial adhesion molecule; VLA-4, very late activating antigen-4; ICAM-1, intercellular adhesion molecule-1.

tion of IFN-γ, $A\beta_{1-42}$, or LPS. Other stimulants for CD40 or combination treatments should be investigated to clarify the involvement of CD40.

We found expression of CD44 on the cell surfaces of both human primary microglial cells and HMO6.N2 cells in the present study. CD44 is a widely expressed cell adhesion molecule in various tissues. The physiological role of CD44 involves cell–cell and cell–matrix adhesion by interaction with hyaluronan (HA), which is a high-molecular-weight polysaccharide found in all tissues of vertebrates. Activated CD44 on the cell surface of leukocytes is thought to contribute to initiate the adhesion and migration of leukocytes in inflammatory brain tissues or stroke (Feuerstein et al., 1998; del Zoppo et al., 2000; Siegelman et al., 2000; Wang et al., 2001). Therefore, we can speculate that CD44 in human microglia also works as an important factor to modify inflammation in injured brain tissues.

PRODUCTION OF CYTOKINES AND CHEMOKINES

There is growing evidence that activated microglia triggered by released stimulants in diseased brains increase the secretion of certain cytokines, which may act harmfully to neurons. Cytokines such as IL-1, IL-6, IFN-γ, TNF-α, and the gram-negative cell wall component LPS increased the release of cytokines from microglial cell lines, including lines of human origin (Righi et al., 1989; Blasi et al., 1990; Atanassov et al., 1995; Speciale et al., 1998; Shigemoto-Mogami et al., 2001; Cheepsunthorn et al., 2001; Rademacher et al., 2004). Although the mechanism of activation remains controversial, induction through MAPK pathways has been studied in the BV-2 murine microglial cell line (Han et al., 2003). Several up-regulated proinflammatory cytokines, such as IL-1β, IL-6, and TNF-α, may orchestrate the responses of the CNS to injury by means of their action, with increased adhesion and migration of inflammatory cells into the CNS and alterations in BBB permeability. As we reported in a previous paper (Nagai et al., 2001b), HMO6.N2 also expressed the gene for the chemokines IL-8, MCP-1, MIP-1α, and MIP-1β, and in fact released IL-8. Microglial cells may respond to chemokines and also play a role in recruitment of leukocytes to focal lesions by releasing such chemokines, as seen in studies with cell lines. With their ease of manipulation, cell lines have been used to elucidate the detailed mechanism of cellular responses under inflammatory conditions. It has been confirmed that matrix metalloproteinases are released from human microglial cell lines under regulation of chemokines (Cross and Woodroofe, 1999), which suggests that chemokines are involved in the breakdown of the BBB. A rat cell line was reported to synthesize multiple cyclooxygenase (COX) products (Rademacher et al., 2004), which may aid in the study of COX-2 and prostanoids in microglia in brain injuries.

There have been many reports discussing expression and release of inducible nitric oxide synthase (iNOS). The expression of iNOS in human microglia is

still a controversial issue (Denis, 1994; Nathan and Xie, 1994; Liu et al., 1996). HA fragments, which are ligands for CD44, induced iNOS expression in the BV-2 murine microglial cell line in a dose-dependent manner, which was increased with IFN-γ (Wang et al., 2004). However, only slight expression of iNOS was detected in HMO6.N2 cells by RT-PCR (data not shown), suggesting that the main source of iNOS might be from other kinds of CNS cells, including astrocytes.

On the contrary, to induce harmful events in the CNS, microglia express the neurotrophins (NT) nerve growth factor (NGF), BDNF, NBT-3, and NT-4/5 as well as their receptors trkA and p75 (Dunn et al., 1987; Shimojo et al., 1991; Araujo and Cotman, 1992a; Mallat and Chamak, 1994; Elkabes et al., 1996), which may contribute to neuronal regeneration. The report for the CHME cell line supported the theory of a cytokine NGF cascade in inflammatory mediator-induced microglial activation and suggested that microglia-derived NGF might function as a signaling molecule between the immune and the nervous systems, directly supporting neuronal survival and/or in directly protecting neurons by antagonizing neurotoxic effects.

Although cell culture studies with primary rodent microglia or human macrophage/monocyte revealed the increased cytokine release following Aβ treatment (Araujo and Cotman, 1992b; Meda et al., 1995; Yan et al., 1996; Fiala et al., 1998), the response of microglia cell lines to Aβ or Aβ fragments is another important issue to be addressed for examining the effect of Aβ in AD. In our study with primary human microglia, treatment with $A\beta_{25-35}$ or $A\beta_{1-42}$ led to increased mRNA levels of IL-8, IL-10, IL-12, TNF-α, MIP-1β, and MCP-1. In HMO6 cells, up-regulation of IL-8, IL-10, IL-12, MIP-1b, and MCP-1 was demonstrated following treatment with $A\beta_{25-35}$ or $A\beta_{1-42}$. ELISA showed that production of IL-1β, IL-8, TNF-α, and MIP-1α increased significantly in primary human microglia following treatment with Aβ. In HMO6 cells, release of IL-8 and TNF-α also increased (Nagai et al., 2001b). In CHME cells, the response to $A\beta_{25-35}$ induced the secretion of NGF. A similar response to Aβ was expected in HMO6.N2 cells as well as primary microglial cells when used in in vitro studies.

MIGRATION OF INTRAVENOUSLY TRANSPLANTED HMO6 CELLS INTO THE MOUSE BRAIN

To test the hypothesis that microglial cells are capable of migration into brain through intact BBB, with their specific phenotype, HMO6 cells were intravenously introduced into adult ICR mice, and their intracerebral migration pattern was determined. HMO6 cells were pulsed for 48 hr with 5 μM 5-bromo-2-deoxyuridine (BrdU) and injected into the jugular vein. Male ICR mice weighing 25–30 g (n = 5; SLC, Hamamatsu, Japan) were anesthetized with 1.0% halothane in 70% N_2O and 30% O_2 with a vaporizer and were subjected to intrajugular vein injections of HMO6 cells. HMO6 cells were suspended at 1×10^7 cells/ml in PBS, and 100 μl of HMO6 suspension was introduced into the left jugular vein with a Hamilton microsyringe. Cyclosporin A (5 mg/kg) was injected intraperitoneally daily as an immunosuppressant. At 5 days posttransplantation, mice were perfused with 4% paraformaldehyde in 0.1 M phosphate buffer. The cryostat sections of the mouse brain were incubated overnight with anti-BrdU antibody (MBL, Nagoya, Japan), followed by biotinylated secondary antibodies and ABC and were visualized with 3,3′-diaminobenzidine (DAB).

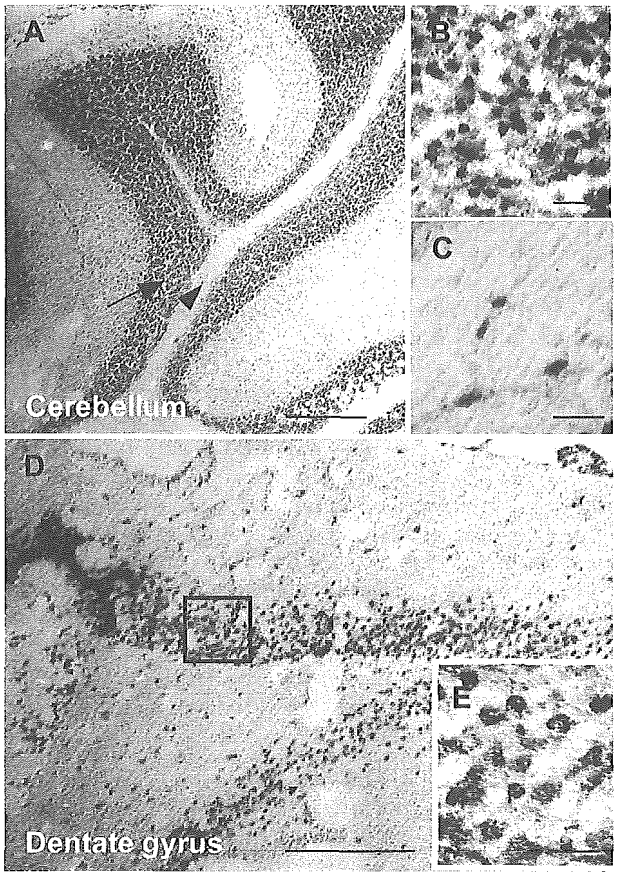

Fig. 3. Immunohistochemical analysis of BrdU labeled cells in HMO6 cells grafted mouse brain.

At 1 day posttransplantation, HMO6 cells had already migrated diffusely into the whole brain and had settled there even at day 7 posttransplantation. HMO6 cells migrated extensively in the brain and were abundant in the region of olfactory bulbs, hippocampus, and cerebellum (Fig. 3).

BrdU-positive cells were also found in the cerebral cortex, basal ganglia, corpus callosum, and brainstem. The overall distribution of HMO6 cells was essentially identical in all animals examined histologically. When the migration of HMO6 cells was examined throughout the body, BrdU-positive cells were also diffusely present in the lung, liver, and spleen.

HMO6 human microglial cells appear to have enough tools to enter the CNS through brain endothelial cells. Primary human microglia and the HMO6 human microglia cell line express CD11b (αMβ2 integrin), CD49b (α2β1 integrin), 49d (α4β1 integrin), and CD49e (α5β1 integrin) as demonstrated by immunocytochemistry and FACS. Integrins expressed on the surface of HMO6 cells appear to represent an important group of molecules that influence extravasation and migration of these cells into the brain. A previous report has indicated that the intraarterially injected Ra2 mouse microglial cell line selectively migrated into the brain (Sawada et al., 1998). The two reports suggest that microglia cell lines represent a useful vehicle for gene transfer into the brain, in that the cells are capable of migrating into the CNS, unlike other cell types that are unable to pass beyond BBB. More detailed studies on microglial migration are underway in our laboratory, but it should be clarified whether intracerebrally migrated microglial cells produce unintended consequences of the immune response resulting from their role as the APCs.

Because previous studies have demonstrated that integrins are involved in maturation of T cells, lymphocyte recirculation, and humoral immune responses to foreign antigens, in addition to cellular migration and homing (Clark et al., 1992; Oostendorp and Dormer, 1997; Ullrich et al., 2001), they are important for antigen presentation, the inflammatory reaction, and migration. Insofar as the CD13/aminopeptidase N is expressed on cells of the myelomonocyte lineage, including myelomonocyte precursors, monocytes, basophils, eosinophils, neutrophils, and myeloid leukemia cells (Look et al., 1989; Miller et al., 1994), expression of CD13 by HMO6 cells indicates that the cell line originated from human microglia of the myelomonocyte lineage.

CONCLUSIONS

The similarities of the human microglial cell line HMO6 and primary human microglia in the phenotype, receptor expression, cytokine production, and migration ability indicate that the stable human microglia cell line HMO6 cell shows great potential as a useful research tool not only for studies of human microglial biology but also for research in human CNS diseases such as MS and stroke, brain injuries, and neurodegenerative diseases in which microglial activation is prominent in the pathophysiology.

REFERENCES

Araujo DM, Cotman CW. 1992a. Basic FGF in astroglial, microglial, and neuronal cultures: characterization of binding sites and modulation of release by lymphokines and trophic factors. J Neurosci 12:1668–1678.

Araujo DM, Cotman CW. 1992b. Beta-amyloid stimulates glial cells in vitro to produce growth factors that accumulate in senile plaques in Alzheimer's disease. Brain Res 569:141–145.

Atanassov CL, Muller CD, Dumont S, Rebel G, Poindron P, Seiler N. 1995. Effect of ammonia on endocytosis and cytokine production by immortalized human microglia and astroglia cells. Neurochem Int 27:417–424.

Blasi E, Barluzzi R, Bocchini V, Mazzolla R, Bistoni F. 1990. Immortalization of murine microglial cells by a v-raf/v-myc carrying retrovirus. J Neuroimmunol 27:229–237.

Briers TW, Desmaretz C, Vanmechelen E. 1994. Generation and characterization of mouse microglial cell lines. J Neuroimmunol 52:153–164.

Bright JJ, Natarajan C, Sriram S, Muthian G. 2004. Signaling through JAK2-STAT5 pathway is essential for IL-3-induced activation of microglia. Glia 45:188–196.

Bruce-Keller AJ, Barger SW, Moss NI, Pham JT, Keller JN, Nath A. 2001. Pro-inflammatory and pro-oxidant properties of the HIV protein Tat in a microglial cell line: attenuation by 17 beta-estradiol. J Neurochem 78:1315–1324.

Cheepsunthorn P, Radov L, Menzies S, Reid J, Connor JR. 2001. Characterization of a novel brain-derived microglial cell line isolated from neonatal rat brain. Glia 35:53–62.

Clark BR, Gallagher JT, Dexter TM. 1992. Cell adhesion in the stromal regulation of haemopoiesis. Baillieres Clin Haematol 5:619–652.

Corradin SB, Mauel J, Donini SD, Quattrocchi E, Ricciardi-Castagnoli P. 1993. Inducible nitric oxide synthase activity of cloned murine microglial cells. Glia 7:255–262.

Cross AK, Woodroofe MN. 1999. Chemokines induce migration and changes in actin polymerization in adult rat brain microglia and a human fetal microglial cell line in vitro. J Neurosci Res 55:17–23.

del Zoppo G, Ginis I, Hallenbeck JM, Iadecola C, Wang X, Feuerstein GZ. 2000. Inflammation and stroke: putative role for cytokines, adhesion molecules and iNOS in brain response to ischemia. Brain Pathol 10:95–112.

Denis M. 1994. Human monocytes/macrophages: NO or no NO? J Leukoc Biol 55:682–684.

Dunn DE, Herold KC, Otten GR, Lancki DW, Gajewski T, Vogel SN, Fitch FW. 1987. Interleukin 2 and concanavalin A stimulate interferon-gamma production in a murine cytolytic T cell clone by different pathways. J Immunol 139:3942–3948.

Elkabes S, DiCicco-Bloom EM, Black IB. 1996. Brain microglia/macrophages express neurotrophins that selectively regulate microglial proliferation and function. J Neurosci 16:2508–2521.

Feuerstein GZ, Wang X, Barone FC. 1998. The role of cytokines in the neuropathology of stroke and neurotrauma. Neuroimmunomodulation 5:143–159.

Fiala M, Zhang L, Gan X, Sherry B, Taub D, Graves MC, Hama S, Way D, Weinand M, Witte M, Lorton D, Kuo YM, Roher AE. 1998. Amyloid-beta induces chemokine secretion and monocyte migration across a human blood–brain barrier model. Mol Med 4:480–489.

Flaris NA, Densmore TL, Molleston MC, Hickey WF. 1993. Characterization of microglia and macrophages in the central nervous system of rats: definition of the differential expression of molecules using standard and novel monoclonal antibodies in normal CNS and in four models of parenchymal reaction. Glia 7:34–40.

Han IO, Kim HS, Kim HC, Joe EH, Kim WK. 2003. Synergistic expression of inducible nitric oxide synthase by phorbol ester and interferon-gamma is mediated through NF-kappaB and ERK in microglial cells. J Neurosci Res 73:659–669.

Hosaka Y, Kitamoto A, Shimojo M, Nakajima K, Imai Y, Handa H, Kohsaka S. 1992. Generation of microglial cell lines by transfection with simian virus 40 large T gene. Neurosci Lett 141:139–142.

Janabi N, Peudenier S, Heron B, Ng KH, Tardieu M. 1995. Establishment of human microglial cell lines after transfection of primary cultures of embryonic microglial cells with the SV40 large T antigen. Neurosci Lett 195:105–108.

Karmann K, Hughes CC, Schechner J, Fanslow WC, Pober JS. 1995. CD40 on human endothelial cells: inducibility by cytokines and functional regulation of adhesion molecule expression. Proc Natl Acad Sci U S A 92:4342–4346.

Kreutzberg GW. 1996. Microglia: a sensor for pathological events in the CNS. Trends Neurosci 19:312–318.

Liu J, Zhao ML, Brosnan CF, Lee SC. 1996. Expression of type II nitric oxide synthase in primary human astrocytes and microglia: role of IL-1beta and IL-1 receptor antagonist. J Immunol 157:3569–3576.

Look AT, Ashmun RA, Shapiro LH, Peiper SC. 1989. Human myeloid plasma membrane glycoprotein CD13 (gp150) is identical to aminopeptidase N. J Clin Invest 83:1299–1307.

Mallat M, Chamak B. 1994. Brain macrophages: neurotoxic or neurotrophic effector cells? J Leukoc Biol 56:416–422.

McGeer PL, Kawamata T, Walker DG, Akiyama H, Tooyama I, McGeer EG. 1993. Microglia in degenerative neurological disease. Glia 7:84–92.

McLaurin J, Almazan G, Williams K, Antel JP. 1995. Immortalization and characterization of rat microglial cells. Neuropathol Appl Neurobiol 21:302–311.

Meda L, Cassatella MA, Szendrei GI, Otvos L Jr, Baron P, Villalba M, Ferrari D, Rossi F. 1995. Activation of microglial cells by beta-amyloid protein and interferon-gamma. Nature 374:647–650.

Miller BC, Ackroyd A, Hersh LB, Cottam GL. 1994. Methionine enkephalin metabolism by murine macrophage ectopeptidase(s). Regul Pept 50:87–98.

Nagai A, Nakagawa E, Choi HB, Hatori K, Kobayashi S, Kim SU. 2001a. Erythropoietin and erythropoietin receptors in human CNS neurons, astrocytes, microglia and oligodendrocytes grown in culture. J Neuropathol Exp Neurol 60:386–392.

Nagai A, Nakagawa E, Hatori K, Choi HB, McLarnon JG, Lee MA, Kim SU. 2001b. Generation and characterization of immortalized human microglial cell lines: expression of cytokines and chemokines. Neurobiol Dis 8:1057–1068.

Nathan C, Xie QW. 1994. Regulation of biosynthesis of nitric oxide. J Biol Chem 269:13725–13728.

Ohsawa K, Imai Y, Nakajima K, Kohsaka S. 1997. Generation and characterization of a microglial cell line, MG5, derived from a p53-deficient mouse. Glia 21:285–298.

Oostendorp RA, Dormer P. 1997. VLA-4-mediated interactions between normal human hematopoietic progenitors and stromal cells. Leuk Lymphoma 24:423–435.

Perry VH, Gordon S. 1991. Macrophages and the nervous system. Int Rev Cytol 125:203–244.

Rademacher DJ, Kearn CS, Carrier EJ, Patel S, Delgado MA, Barkmeier A, Klick DE, Breese NM, Pfister SL, Nithipatikom K, Campbell WB, Hillard CJ. 2004. Production of hydroxyeicosatetraenoic acids and prostaglandins by a novel rat microglial cell line. J Neuroimmunol 149:130–141.

Righi M, Mori L, DeLibero G, Sironi M, Biondi A, Mantovani A, Denis-Donini S, Ricciardi-Castagnoli P. 1989. Monokine production by microglial cell clones. Eur J Immunol 19:1443–1448.

Rio-Hortega PD. 1932. Microglia. In: Penfield W, editor.Cytology and cellular pathology of nervous system, vol 2. New York: Paul B. Hoeber. p 481–534.

Satoh J, Kim SU. 1994. Differential expression of Lewis(x) and sialyl-Lewis(x) antigens in fetal human neural cells in culture. J Neurosci Res 37:466–474.

Sawada M, Imai F, Suzuki H, Hayakawa M, Kanno T, Nagatsu T. 1998. Brain-specific gene expression by immortalized microglial cell-mediated gene transfer in the mammalian brain. FEBS Lett 433:37–40.

Sempowski GD, Chess PR, Phipps RP. 1997. CD40 is a functional activation antigen and B7-independent T cell costimulatory molecule on normal human lung fibroblasts. J Immunol 158:4670–4677.

Shigemoto-Mogami Y, Koizumi S, Tsuda M, Ohsawa K, Kohsaka S, Inoue K. 2001. Mechanisms underlying extracellular ATP-evoked interleukin-6 release in mouse microglial cell line, MG-5. J Neurochem 78:1339–1349.

Shimojo M, Nakajima K, Takei N, Hamanoue M, Kohsaka S. 1991. Production of basic fibroblast growth factor in cultured rat brain microglia. Neurosci Lett 123:229–231.

Shrikant P, Benveniste EN. 1996. The central nervous system as an immunocompetent organ: role of glial cells in antigen presentation. J Immunol 157:1819–1822.

Siegelman MH, Stanescu D, Estess P. 2000. The CD44-initiated pathway of T-cell extravasation uses VLA-4 but not LFA-1 for firm adhesion. J Clin Invest 105:683–691.

Speciale L, Roda K, Saresella M, Taramelli D, Ferrante P. 1998. Different endothelins stimulate cytokine production by peritoneal macrophages and microglial cell line. Immunology 93:109–114.

Suzumura A, Mezitis SG, Gonatas NK, Silberberg DH. 1987. MHC antigen expression on bulk isolated macrophage-microglia from newborn mouse brain: induction of Ia antigen expression by gamma-interferon. J Neuroimmunol 15:263–278.

Tan J, Town T, Paris D, Mori T, Suo Z, Crawford F, Mattson MP, Flavell RA, Mullan M. 1999. Microglial activation resulting from CD40-CD40L interaction after beta-amyloid stimulation. Science 286:2352–2355.

Ullrich O, Diestel A, Eyupoglu IY, Nitsch R. 2001. Regulation of microglial expression of integrins by poly(ADP-ribose) polymerase-1. Nat Cell Biol 3:1035–1042.

Walker WS, Gatewood J, Olivas E, Askew D, Havenith CE. 1995. Mouse microglial cell lines differing in constitutive and interferon-gamma-inducible antigen-presenting activities for naive and memory $CD4^+$ and $CD8^+$ T cells. J Neuroimmunol 63:163–174.

Wang H, Zhan Y, Xu L, Feuerstein GZ, Wang X. 2001. Use of suppression subtractive hybridization for differential gene expression in stroke: discovery of CD44 gene expression and localization in permanent focal stroke in rats. Stroke 32:1020–1027.

Wang MJ, Jeng KC, Kuo JS, Chen HL, Huang HY, Chen WF, Lin SZ. 2004. c-Jun N-terminal kinase and, to a lesser extent, p38 mitogen-activated protein kinase regulate inducible nitric oxide synthase expression in hyaluronan fragments-stimulated BV-2 microglia. J Neuroimmunol 146:50–62.

Yan SD, Chen X, Fu J, Chen M, Zhu H, Roher A, Slattery T, Zhao L, Nagashima M, Morser J, Migheli A, Nawroth P, Stern D, Schmidt AM. 1996. RAGE and amyloid-beta peptide neurotoxicity in Alzheimer's disease. Nature 382:685–691.

総説

脳卒中標準データベースの有用性

小林祥泰

Usefulness of Japanese Standard Stroke Database

by

Shotai Kobayashi, M.D., and Japan Standard Stroke Registry Study (JSSRS) Group

from

Department of Neurology, Hematology & Rheumatology, Shimane University, School of Medicine

The Japan Standard Stroke Registry Study (JSSRS) Group, is creating a permanent national acute stroke databank using an international stroke evaluation index. We analysed ultra acute thrombolytic therapy for ischemic stroke. Our data suggests that thrombolysis is effective in acute ischemic stroke in Japan. Concerning brain hemorrhage, our data shows that significantly better results were obtained from selectivery operated patients. The JSSRS system is basically working as a self computed database for acute stroke hospitals. Therefore, this database can help to confirm statistical data concerning patients and provide to make compaisions with other hospitals or Japanese data easily. It may also be a great help for preparing original data for informed consent and for information on hospital stroke therapy.

(Received July 22, 2004; accepted August 17, 2004)

Key words : stroke databank, outcome study, t-PA, Asian stroke research, Japan Standard Stroke Registry Study (JSSRS)

Jpn J Neurosurg (Tokyo) 14 : 3-9, 2005

脳卒中データバンク

脳卒中データバンクのコンセプトは，1）診断基準統一，2）重症度評価標準化，3）アウトカムスケール標準化，4）各病院のデータベースとしての機能，5）日本におけるデータ集計が可能，6）諸外国や他施設との比較が可能となることである．

著者らは，わが国における脳卒中の実態調査を継続的に行うデータバンク構築を目指して，1999～2002年に厚生科学研究事業による脳卒中急性期患者データベース構築研究(Japan Standard Stroke Registry Study; JSSRS)[1]を行い，脳卒中病型診断〔National Institute of Neurological Disorders and Stroke (NINDS) の脳卒中III分類〕，重症度評価〔National Institude of Neurological Stroke Scale (NIHSS) および Japan Stroke Scale (JSS)〕，アウトカムスケール〔modified Rankin Scale (mRS)〕などを国際標準化し，各病院のデータベースとして使用できるコンピュータベースの脳卒中急性期患者データベースシステムを構築した．班研究終了後からは，日本脳卒中協会データバンク部門として登録事業を継続している．

現在の参加施設は，班研究終了時の47施設から100施設以上に増加し，日本の脳卒中データベースの標準となりつつある．2002年度までの解析結果は『脳卒中データバンク2003』(中山書店) として2003年3月に出版されている．また，班研究成果およびその後の学会発表などの要旨が，脳卒中データバンクホームページ

島根大学医学部神経・血液・膠原病内科／〒693-8501 出雲市塩冶町89-1〔連絡先：小林祥泰〕
Address reprint requests to: Shotai Kobayashi, M.D., Department of Neurology, Hematology & Rheumatology, Shimane University, School of Medicine 89-1 Enya-cho, Izumo-shi, Shimane 693-8501, Japan

(http://cvddb.med.shimane-u.ac.jp/) に掲載されているので，興味のある方は参照していただきたい．2005 年には『脳卒中データバンク 2005』を出版予定である．また今後，PDA 版のソフト開発，電子カルテとの連携システムの開発を進めていく予定である．

脳卒中の病型別頻度および危険因子

JSSRS2004 では，脳卒中全体（16,992 例）に占める脳梗塞病型別頻度でも **Fig. 1** のようにアテローム血栓性梗塞（血管-血管塞栓のアテローム血栓性塞栓も含む）が 24.3% とラクナ梗塞の 23.5% を上回り，心原性脳塞栓も 19% とラクナ梗塞に近づいていた．アテローム血栓性梗塞においても高血圧が重要な因子であるので，脳卒中に対する最大の危険因子であることは変わりないが，ラクナ梗塞が 40% 以上を占めていた以前と比較すると日本人の脳卒中病型の分布が異なってきており，より欧米型に近づいている印象がある．高血圧性脳出血は 12.1%，クモ膜下出血（subarachnoid hemorrhage；SAH）は 5.5% であった．

危険因子についてみると，脳卒中全体（平均年齢 69 歳）における高血圧の頻度は 63% と，喫煙 30%，糖尿病 23%，高脂血症 23%，心房細動 19%，飲酒毎日 2 合以上 9%，脳卒中家族歴 20% に比し最も頻度が高かった[2]．

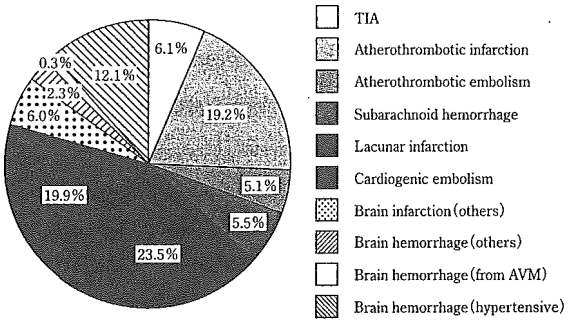

Fig. 1　Incidence of stroke by type (JSSRS2003, $n=16,992$)[4]

病型別にみた脳卒中の年代分布

病型別にどの年代にピークがあるかをみてみると，**Table 1** のようにアテローム血栓性梗塞，ラクナ梗塞は 70 代がピークであるが，心原性脳塞栓は 70～80 歳でピークとなっており高齢者に多いことを示している．出血性脳卒中のピークは脳梗塞よりも若年であった．今後さらに高齢化が進めば，ますます心原性脳塞栓の頻度が増加することが予想され，要介護となる後遺症増加に対する配慮が必要となる．

病型別にみた発症-来院時間

JSSRS2001 の脳梗塞 5,405 例における集計では，発症 3 時間以内の来院例は 38% で，発症 6 時間以内を合わせると半数であった．これは全国 16,000 例の脳梗塞を集計した山口[3]の報告と一致していた．すなわち，比較的多くの例が血栓溶解療法の適応となる 3 時間以内に来院していることがうかがわれ，近い将来，わが国で組み替え組織プラスミノゲンアクチベーター（t-PA）が認可された際には，brain attack キャンペーンなどにより超急性期来院例がさらに増加すると予測される．今後は地域脳卒中拠点病院のように，t-PA 治療を実施する病院をある程度センター化して，適応例を多く集め効率よく治療する方策を考えていく必要がある．また，発症-来院時間に僅かながら地域差もあり，関東地区では比較的時間がかかっている傾向が認められた．

Table 1　Incidence (%) of stroke subtype according to age (JSSRS2002, n=16,992)

	<50 years	50-59 years	60-69 years	70-79 years	80 years≦
TIA	6.994	15.179	27.976	31.994	17.857
Atherothrombotic infarction	3.389	13.202	26.909	33.789	22.711
Atherothrombotic embolism	2.467	8.729	25.996	39.089	23.719
Subarachnoid hemorrhage	18.341	25.359	23.604	21.531	11.164
Lacunar infarction	3.670	17.732	28.701	32.041	17.856
Cardiogenic embolism	3.231	8.300	21.223	36.531	30.716
Brain infarction (others)	17.091	13.636	23.091	28.909	17.273
Brain hemorrhage (others)	13.566	14.341	20.155	31.395	20.543
Brain hemorrhage (from AVM)	54.286	22.857	8.571	14.286	0.000
Brain hemorrhage (hypertensive)	9.005	22.396	29.287	25.607	13.704
Total	6.361	15.164	25.907	31.931	20.673

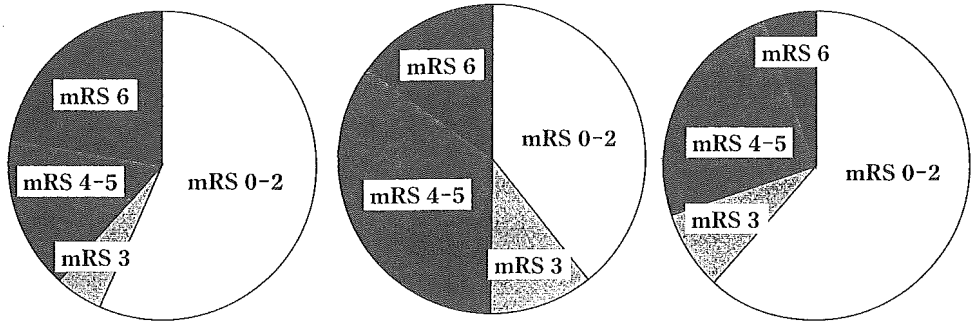

Subarachnoid hemorrhage $n=458$ | Hypertensive brain hemorrhage $n=918$ | Ischemic stroke $n=5,765$

Fig. 2 Prognosis at hospital discharge for stroke by type (modified Rankin scale) (JSSRS 2001)[4]

急性期脳卒中の病型別退院時予後

JSSRS による mRS でみた病型別退院時予後を **Fig. 2** に示す．SAH では死亡率は高いが寝たきりは少なく，比較的軽症で，手術施行症例は予後が良好なことを示している．当然のことながら，入院時の Hunt & Kosnik の SAH 重症度と mRS は逆相関を示していた．高血圧性脳出血は昔に比べて激減したとはいえ，SAH について死亡率が高く，寝たきりになる率も高い予後不良の病型である．脳梗塞では死亡率は低いが寝たきりになる頻度はかなり高い．その大半は高齢者の心原性脳塞栓によるものである．心原性脳塞栓では寝たきりおよび死亡が 30%に及び，予後不良（mRS：5-6）な脳梗塞の実に 51%を心原性脳塞栓が占めていた[2]．

心房細動があれば当然抗凝固療法の適応となるが，抗凝固・血小板療法の有無でみた高血圧性脳出血の退院時予後について調べてみると，発症前に抗凝固・血小板療法施行群で有意に死亡率が高いことが判明した[4]．以前から，抗血小板薬服用例では，血腫が進行性に拡大する例があるという印象を持っていたが，今回の集計でそのことが裏づけられた．最近では MRI T2*撮像法が普及し，潜在性小出血も診断できるようになってきたので，潜在性小出血が多発するような典型的なラクナ梗塞では，抗血小板薬よりも高血圧の管理を十分に行うことが重要である．

超急性期血栓溶解療法の実施頻度と退院時予後

Brain attack とは発症 3 時間以内の可及的速やかな血栓溶解療法が行われることを前提とした言葉である．どんなに早く来院しても，この治療なくしては治療効果は運任せである．米国では血栓溶解療法の啓蒙キャンペーンを大々的に行い，最近の米国の脳卒中センター共同研究の 6,000 例の集計では，t-PA 投与率は適応例全体の 4.6%であるが，発症 1 時間以内脳梗塞入院例では 58.6%にも達していると報告されている[5]．わが国ではいまだ脳梗塞に対する t-PA の保険適応は認められていないが，JSSRS の集計によると t-PA や大量ウロキナーゼ（UK）の動注，静注を含めた血栓溶解療法は治療法の記載のある脳梗塞 5,874 例中 226 例（3.8%）に施行されており，発症 3 時間以内で中等症の 665 例に限ると 15.5%の例で施行されていた[6]．静注 t-PA の効果が非常に大きいのはやはり発症 1 時間以内であり[7]，わが国においても救急隊と連携してこの超急性期脳梗塞例を増やす努力が必要である．JSSRS による血栓溶解療法の retrospective 解析でも，**Fig. 3** のように mRS 0-1 と社会復帰可能な例が 32%と対照群の 20%に比し，高率であった[6]．対照群において発症 3 カ月後の予後についても調査したが，mRS 0-1 は 21%とほぼ同様の結果であった[8]．米国の t-PA の臨床試験よりは mRS 0-1 比率が両群とも低めであるが，米国の試験と異なり NIHSS で 6-29 の中等-重症例を選択していることが影響しているものと思われる．

JSSRS2003 による集計では t-PA 静注が 99 例に行われていたので，血栓溶解療法を内容別に分けて，実施された全例について予後を検討してみた．**Fig. 4** に示すように t-PA 静注投与群で退院時 mRS 0-1 が 37%と最も高く，また死亡率も最も低かった．この結果は t-PA のオープン試験の成績ときわめて類似した結果であり，十分適応を考慮したうえで使用される t-PA 静注投与は，比較的安定した効果と安全性を示すことを示唆するもの